J. Physiol. (1985), **365**, *pp.* 331–363
With 16 *text-figures*
Printed in Great Britain

SPATIAL AND TEMPORAL FREQUENCY SELECTIVITY OF NEURONES IN VISUAL CORTICAL AREAS V1 AND V2 OF THE MACAQUE MONKEY

BY KENT H. FOSTER*, JAMES P. GASKA*, MIRIAM NAGLER† AND DANIEL A. POLLEN*

From the Division of Neurobiology, Barrow Neurological Institute, Phoenix, AZ 85013, U.S.A. and the Department of Neurology, University of Massachusetts Medical School, Worcester, MA 01605, U.S.A.

(*Received 8 June 1984*)

SUMMARY

1. The spatial and temporal frequency selectivity of 148 neurones in the striate cortex, V1, and of 122 neurones in the second visual cortical area, V2, of the macaque monkey were studied using sine-wave gratings of suprathreshold contrast drifting over the receptive field at the preferred orientation and direction.

2. Neurones in V1 and V2 were selective for different but partially overlapping ranges of the spatial frequency spectrum. At retinal eccentricities of 2–5 deg from the fovea, the spatial frequency preferences for neurones ranged from 0·5 to 8·0 cycles/deg in V1 and from 0·2 to 2·1 cycles/deg in V2 and were on average almost 2 octaves lower in V2 than in V1. Spatial frequency full band widths in the two cortical areas were in the range 0·8–3·0 octaves, with a mean value of 1·8 octaves, in the parafoveal representation of both V1 and V2, and 1·4 and 1·6 octaves respectively in the foveal representation of V1 and V2.

3. Most neurones in V1 and some in V2 responded well at temporal frequencies up to 5·6–8·0 Hz before their responses dropped off at still higher frequencies. In V1, 68 % of the neurones exhibited low-pass temporal tuning characteristics and 32 % were very broadly tuned, with a mean temporal frequency full band width of 2·9 octaves. However, in V2 only 30 % of the neurones showed low-pass temporal selectivity and 70 % of the cells had bandpass temporal characteristics, with a mean full band width of 2·1 octaves. In V2 the minimal overlap of bandpass tuning curves across the temporal frequency spectrum suggests that there are at least two distinct bandpass temporal frequency mechanisms as well as neurones with low-pass temporal frequency tuning at each spatial frequency.

4. A matrix of spatial and temporal frequency combinations was employed as stimuli for neurones with bandpass temporal frequency selectivity in both V1 and V2. The resultant spatio-temporal surfaces provided evidence that a neurone's preference

* Present address: Department of Neurology, University of Massachusetts Medical School, Worcester, MA 01605, U.S.A.

† Present address: Department of Applied Mathematics, The Weizmann Institute of Science, Rehovot 76100, Israel.

for spatial frequency is essentially independent of the test temporal frequency; however, in V2 there was some tendency for temporal frequency peaks to shift slightly towards lower frequencies when non-optimum values of spatial frequency either above or below the preferred value were tested.

5. Neurones with pronounced directional selectivity were encountered over a wide range of spatial frequencies, although in both cortical areas there was a tendency for an increased incidence of directional selectivity among neurones which were selective for lower spatial frequencies and higher temporal frequencies.

6. These results indicate that neurones in V1 and V2 span partially overlapping but essentially different ranges of the spatial frequency spectrum yet have similar spatial frequency band widths, whereas neurones in V1 and V2 span similar ranges of the temporal frequency spectrum but have different temporal frequency bandpass characteristics. Taken together, neurones in V1 and V2 analyse spatially localized subdomains of the visual scene across an extended range of both the spatial frequency and temporal frequency spectrum.

INTRODUCTION

The rationale for determining the spatial and temporal frequency selectivity of central visual neurones is well understood (Robson, 1975; Braddick, Campbell & Atkinson, 1978). Many investigators have studied the spatial frequency selectivity of neurones in area 17 of the cat and have considered their results in terms of various models proposed to account for the capabilities of the visual system with respect to spatial pattern recognition (for recent review, see Pollen & Ronner, 1983). Several groups have also studied the spatial frequency selectivity of neurones in the striate cortex, V1, of the macaque monkey (Schiller, Finlay & Volman, 1976*a*; DeValois, Albrecht & Thorell, 1982). Such studies in the macaque are particularly relevant for understanding spatial vision in man because the contrast sensitivity functions in the two species are almost identical (DeValois, Morgan & Snodderly, 1974).

The issue of temporal frequency selectivity of neurones in area 17 (or V1) of the cat has been addressed (Ikeda & Wright, 1975; Movshon, Thompson & Tolhurst, 1978*a*, Holub & Morton-Gibson, 1981; Berardi, Bisti, Cattaneo, Fiorentini & Maffei, 1982), but as yet there has been no comparable study in the macaque monkey. Such studies would be of interest in view of the extensive psychophysical literature on this subject in man (Kelly & Burbeck, 1984). At present there have been no reported studies of the spatial and temporal frequency characteristics of neurones in V2 of the macaque monkey, even though these questions have been investigated in area 18 (or V2) of the cat (Movshon *et al.* 1978*a*; Berardi *et al.* 1982). However, species differences between cat and monkey with respect to both the pattern of thalamo-cortical projections to V2 (Hendrickson, Wilson & Ogren, 1978) and the dependence of neuronal activity of V2 on the physiological integrity of V1 (Schiller & Malpeli, 1977) suggest the necessity for an independent investigation in the macaque monkey.

Such studies in V2 in the macaque monkey are of particular interest because V2 is the first of the extrastriate areas, is the only one of comparable size to V1 (Gattass, Gross & Sandell, 1981; Weller & Kaas, 1983) and has been identified in every mammalian species thus far studied (Allman & Kaas, 1974). Moreover, V2 not only

receives a dense projection of cortical efferents from V1 (Lund, Hendrickson, Ogren & Tobin, 1981) but is itself a source of major projections to higher extrastriate cortical areas (Desimone, Fleming & Gross, 1980; Rockland & Pandya, 1981; Maunsell & Van Essen, 1983).

Hence the present studies have been undertaken to close a gap in our understanding of the spatial and temporal frequency-selective properties neurones in V1 and V2 of the macaque monkey.

METHODS

Surgical and anaesthetic procedures. Experiments were performed on male macaque monkeys (*Macaca fascicularis*) weighing 2·5–3 kg prepared for chronic studies. At least 1 week prior to the first experimental session, surgery was performed under deep general anaesthesia (pentobarbitone, 35 mg/kg). In addition, a long-acting local anaesthetic was injected into the scalp prior to the incision. Two Kopf cylinders were then attached to the skull using dental acrylic cement so that the animal could later be painlessly positioned in the stereotaxic apparatus during experiments. A trephine hole was made over the recording site, and a stainless-steel chamber was placed over the trephine hole and secured with dental acrylic cement. The recording chamber was filled with an antibiotic ointment (gentamicin sulphate) and a stainless-steel cap was screwed in place over the chamber. Post-operatively, the animals received injections of a narcotic analgesic (meperidine hydrochloride, 1 mg/kg) thrice-daily for 3 days following surgery.

On experimental days a short acting barbiturate (methohexital sodium, 3 mg/kg, I.V.) was slowly injected via an intravenous canula until general anaesthesia was induced. Paralysis was initially produced using gallamine triethiodide (2·0 mg/kg, I.V.) followed by endotracheal intubation under the general anaesthesia. The animal was then respirated on a mixture of 70% nitrous oxide and 30% oxygen for light anaesthesia and analgesia at a rate resulting in P_{CO_2} levels of 4·2–4·8%. No ear, eye or mouth bars were used, and great care was always taken to eliminate all possible sources of discomfort or pain. The e.e.g. and e.c.g. were monitored and supplementary sodium pentobarbitone was available for intravenous injection and given as needed. Body temperature was restricted to normal limits by a thermostatically controlled heating pad. Paralysis was maintained throughout the experiment by a continuous infusion of 5% dextrose in saline and pancuronium bromide (0·2 mg/kg . h). At the end of non-terminal experiments the pancuronium bromide was discontinued, and as soon as the animal regained some muscle tone the residual paralysis was reversed by slow injection of a mixture of physostigmine and atropine. Each such experiment required about 2 h set-up time, 12 h recording time and about 2 h for reversal of the paralysis. As soon as the animals were competent to maintain postural control they were returned to their cages and resumed their usual activities within a short period of time.

Optics. Cyclopentolate hydrochloride was used for cycloplegia and mydriasis. Gas-permeable hard contact lenses were selected by retinoscopy, and artificial pupils (3 mm in diameter) were then placed over each lens. Refraction was further corrected to $\frac{1}{4}$ dioptre by adjusting trial lenses until the response of a neurone to a very high spatial frequency grating was maximal.

Recording techniques. Electrodes were either tungsten in parylene (Bak Electronics) or (more often) platinum–iridium-in-glass electrodes which were fabricated in our laboratory. Exposed tip sizes were 10–15 μm in length and 5–7 μm in width at the base. Standard techniques of amplification, filtering, and spike discrimination were employed. Digitized output from a window discriminator, representing the action potentials of a single neurone, was fed to an Apple II Plus computer for on-line data analysis. Every effort was made to complete a penetration through all the laminae of either V1 or V2 in a given experiment so that our cell population reflected an evenly sampled distribution from each cortex.

Cell assignment and histological confirmation. The maps of Talbot & Marshall (1941) and Daniel & Whitteridge (1961) were used for identification of V1. During each experiment we used the criteria of Baizer, Robinson & Dow (1977) for tentatively distinguishing neurones in V2 from those in V1. At the end of each experiment, electrode locations were marked by electrolytic lesions. The animal was then killed by an overdose of sodium pentobarbitone and perfused intracardially with normal saline followed by a buffered 10% (w/v) formalin solution. The brain was then placed in

a 30 % sucrose and formalin solution until it sank, then sectioned in 33 μm slices and stained with Cresyl Violet. Because of the long survival times of our animals, successful recovery of the lesions required that they be relatively large (currents were usually 5 μA for 30–45 s, resulting in a lesion diameter of 150–200 μm). In order to avoid current-related damage to the surrounding tissue and to the micro-electrode tip, lesions were made upon withdrawal of the micro-electrode at the end of each penetration. Such lesions reliably distinguished whether the tract was in V1 or V2, but failed to provide precise laminar localization within a cortical area along the full extent of the tract. Only cells which could be unambiguously assigned to either V1 or V2 on the basis of subsequent histological assignment of a micro-electrode track with lesions in most cases, or less often upon identification of the track alone, have been included in this study.

Visual stimulation. Stimuli were presented on the face of Tektronix 608 display monitor with a P4 phosphor. The X, Y and Z inputs to the oscilloscope were taken from the cathode-ray tube image generator (Innisfree, Inc.) under computer control which was used to produce a one dimensional drifting sinusoidal grating or a thin bar of arbitrary orientation and velocity. The mean luminance of the oscilloscope face was 50 cd/m^2. Grating contrast was defined using the Michaelson formula $C_{\text{grating}} = (L_{\max} - L_{\min})/(L_{\max} + L_{\min})$. Bar contrast was defined as the luminance increase (light bar) or luminance decrease (dark bar) of the bar above or below 50 cd/m^2 divided by 50 cd/m^2.

Stimulus presentation. The optimum orientation was determined qualitatively by listening to the cell's response to differently oriented bars or gratings, or by direct quantitative studies. Stimuli were then presented at the optimum orientation to the dominant eye, the other eye being covered.

Presentation of drifting gratings was preceded by a uniform field for 1 s, after which the grating contrast was ramped up from 0 to 0·35 over a 1 s period, held constant for 5 s and ramped down at the same rate. During the 3 s between trials, the spatial frequency or temporal frequency of the grating was changed. A stimulus block consisted of a set of stimulus trials in which all gratings with different spatial and/or temporal frequencies were presented once in random order. The stimulus order was newly randomized for each stimulus block and a neurone's responses to five to ten stimulus blocks were averaged to produce a tuning curve.

For most cells a spatial frequency study was run first using stimulus blocks in which the spatial frequency of the grating was changed between trials while the drift frequency of the grating was held constant, generally at 2–4 Hz. A second study was then run in which the drift frequency was changed while holding the spatial frequency of the grating constant at the previously determined preferred spatial frequency. If, after running a drift frequency study, it was determined that the drift frequency at which the spatial frequency was originally run produced a response which was less than 50 % of the response produced by the preferred drift frequency, then a second spatial frequency study was carried out. All spatial frequency band widths which we report were measured from studies carried out at or close to the optimum drift frequency.

A bar study began by drifting a light bar at the preferred orientation and velocity across the receptive field of the cell in both directions. The contrast polarity of the bar was then reversed from light to dark and the bar was again drifted back and forth across the receptive field. This stimulus cycle was repeated 20–50 times for each cell.

RESULTS

We studied the spatial and temporal frequency selectivity of 130 neurones in the parafoveal representation of V1 and 96 cells in parafoveal V2 at retinal eccentricities of 2–5 deg from the fovea. Additionally, we studied 18 cells in foveal V1 and 26 cells in foveal V2 at a retinal eccentricity of $\leqslant 1$ deg in order to assess any differences in scale factors between the two cortical populations as a function of retinal eccentricity. These 270 neurones were accumulated from thirty successful penetrations made in eight macaque monkeys.

Initial parametric studies. After the preferred orientation of a cell had been determined, a narrow slit, reversing in contrast between trials, was drifted across the receptive field in both directions. For simple cells (Hubel & Wiesel, 1962), the distinct

spatial offset between zones of peak excitation in response to drifting single light and dark bars is apparent (Fig. 1 *A*), as is the distinct directional selectivity preference for the example shown (compare Fig. 1 *A* and *B*).

For complex cells, the zones of increased response to narrow single drifting light and dark bars showed almost complete overlap (Fig. 1 *D* and *E*). The strength of the response to light and dark bars was sometimes equal, sometimes unequal (Fig. 1 *D*

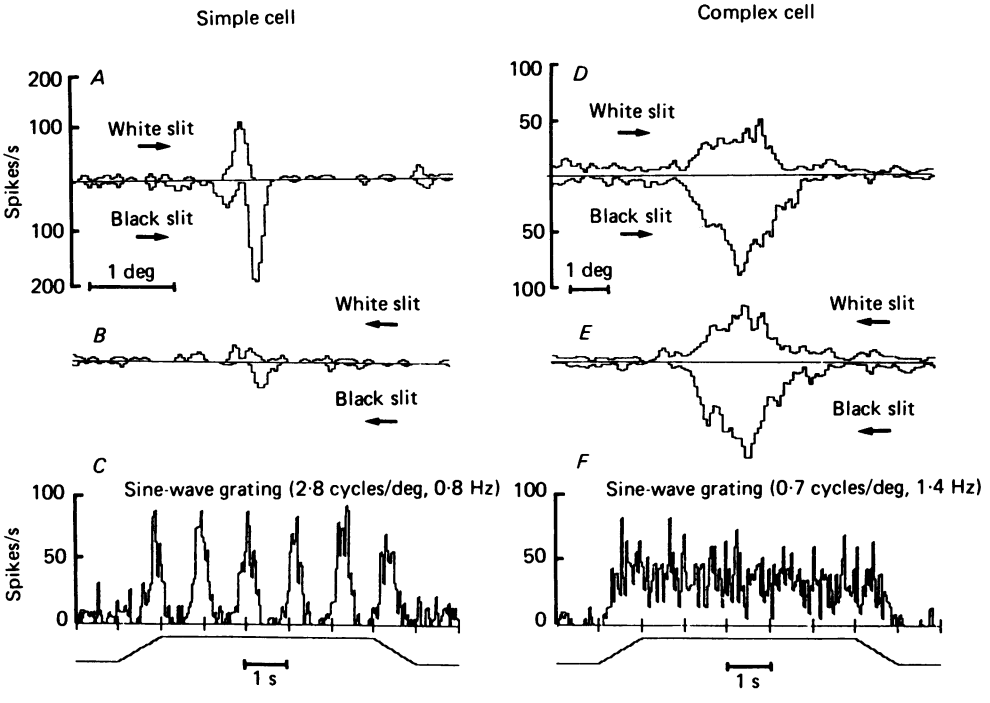

Fig. 1. Responses to a thin bar drifting first in one direction and then in the opposite direction are shown for a simple cell (*A* and *B*) and for a complex cell (*D* and *E*). Both dark and light bars were used. The response to the light bar is plotted above the dividing line. The response to the dark bar is plotted below the dividing line. Responses of the same two cells to a drifting sine-wave grating of the preferred spatial and temporal frequencies are shown in *C* and *F*. The contrast of the grating was ramped up from 0 to 0·30, held constant, and then ramped down to 0. The time course of the contrast is shown by the trace below the histogram. The calibrations in *A* also apply to *B* and the calibrations in *D* also apply to *E*. Bin widths throughout all studies ranged from 25 to 37·5 ms. In this and subsequent illustrations, a cell's response to a grating stimulus was computed by subtracting the mean spikes per second during the spontaneous period (blank period) from the mean spike rate during the 5 s period, in which the contrast of the grating was held constant at 0·35 (on period). Spikes during the 1 s period before the contrast ramp determined the spontaneous activity.

and *E*). The response peaks corresponding to the two directions of movement were measured to assess directional preference. An example of bidirectional selectivity is shown in Fig. 1 *D* and *E*. Receptive field widths were calculated from average response histograms of the type shown in Fig. 1 *A*, *B*, *D* and *E* by measuring the full extent of excitatory activity above the spontaneous firing level to both the light and dark bars.

Responses of simple cells to drifting sine-wave gratings at the preferred spatial frequency were truncated because of the zero firing level (Fig. 1*C*), as previously shown in the cat (Movshon & Tolhurst, 1975; Movshon, Thompson & Tolhurst, 1978*b*; Andrews & Pollen, 1979) and macaque monkey (Schiller *et al.* 1976*a*).

Responses of complex cells to drifting sine-wave gratings at the preferred spatial frequency (Fig. 1*F*) were essentially unmodulated (72% of all cells), as previously shown for the cat (Maffei & Fiorentini, 1973; Movshon, Thompson & Tolhurst, 1978*c*)

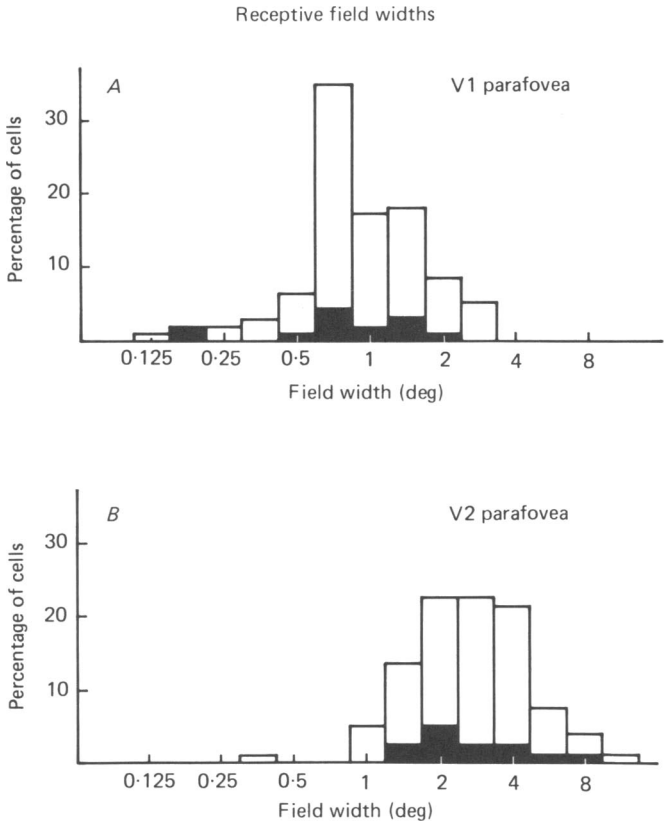

Fig. 2. The distribution of receptive field widths obtained from studies of parafoveal neurones is shown for V1 (*A*) and V2 (*B*). Simple cells are represented by the filled part of the bars, complex cells by the open part of the bars. There is almost a 3-fold increase in the average receptive field size in V2 (mean = 3·0 deg) as compared to V1 (mean = 1·1 deg).

and macaque monkey (Schiller *et al.* 1976*a*), or consisted of a modulated level superimposed upon an unmodulated level (12% of all cells), a response pattern variant for complex cells previously shown in the cat (Pollen, Andrews & Feldon, 1978; Glezer, Tsherbach, Gauselman & Bondarko, 1980; Kulikowski & Bishop, 1982; Dean & Tolhurst, 1983) and macaque monkey (DeValois *et al.* 1982).

Simple cells comprised 14% of the parafoveal population in V1, a percentage slightly higher than the 7–9% range found in several studied (e.g. Hubel & Wiesel,

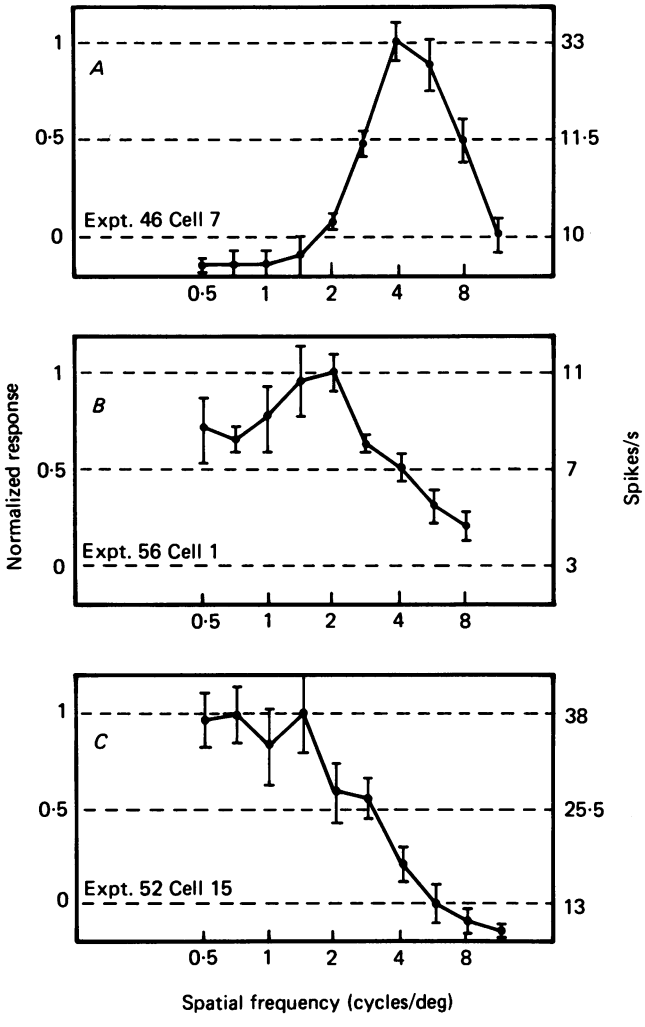

Fig. 3. Spatial frequency tuning curves obtained from three neurones are shown to illustrate the types of curves found in this study: first, those which respond to only a limited range of the spatial frequency spectrum (*A*); secondly, those with a definable peak frequency, but with only modest low frequency response attenuation (*B*); thirdly, those having no identifiable peak frequency because of little or no low frequency attenuation (*C*). For each curve, the maximum response has been normalized to 1·0 on the left side of the vertical axis, with 0·0 representing the spontaneous firing rate. The right side of the vertical axis is scaled in spikes/s. The majority of curves for neurones in V1 and V2 were similar to the example shown in *A*.

1968; Poggio, 1972; Dow, 1974) but lower than the 22% found by Schiller, Finlay & Volman (1976*b*) and substantially lower than the almost 50% figure found by DeValois *et al.* 1982. Simple cells comprised 16% of the parafoveal V2 population.

Receptive field widths of neurones in V1 and V2. Field widths in parafoveal V1 were in the range 0·13–3·0 deg, and widths in V2 were 1–10 deg (Fig. 2), except for a single cell with a field diameter of 0·38 deg. The mean receptive field width of neurones in

parafoveal V1 was $1{\cdot}05 \pm 0{\cdot}06$ deg ($n = 97$), and the mean for neurones V2 at comparable retinal eccentricities was $2{\cdot}97 \pm 0{\cdot}19$ deg ($n = 79$). Thus, there is an almost 3-fold increase in the receptive field width in V2 compared to V1, consistent with previous reports (Baizer *et al.* 1977; Van Essen & Zeki, 1978; Gattass *et al.* 1981). There is no clear trend in terms of differences of receptive fields widths of simple cells (filled bars) and complex cells (open bars) in V1 and V2 (Fig. 2), although the incidence of simple cells in our populations is probably too low for this problem to be resolved.

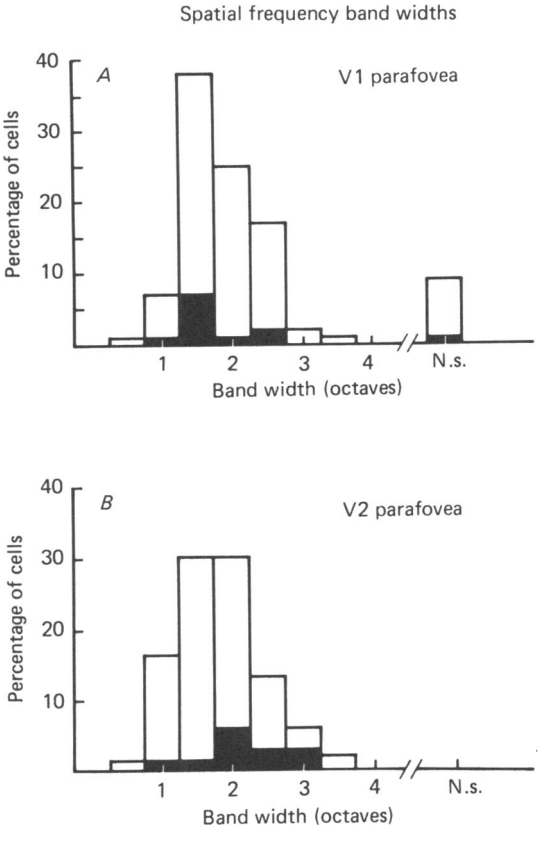

Fig. 4. The distribution of spatial frequency band widths obtained from studies of parafoveal neurones is shown for V1 (*A*) and V2 (*B*). Neurones classified as non-selective for spatial frequency (see examples in Fig. 3*B* and *C*) are labelled as N.s. Simple cells are represented by the filled part of the bars, complex cells by the open part of the bars.

Spatial frequency selectivity of neurones in V1 and V2. Three types of spatial frequency selectivity curves were found (Fig. 3). The majority of curves were bandpass (Fig. 3*A*) with a marked decrease in response to spatial frequencies higher or lower than the optimum frequency. Such curves were found for 91 % of neurones in V1 and 100 % of neurones in determinable cases in V2. For these curves the full band widths were specified in octaves at half-maximal amplitude.

Spatial frequency selectivity curves with shallow low frequency attenuation

(Fig. 3*B*) or almost no low frequency attenuation (Fig. 3*C*) comprised 9% of the parafoveal V1 population. Some of the cells in V2 had preferences for such low spatial frequencies (i.e. $\leqslant 0{\cdot}25$ cycles/deg) that it was not always technically feasible to measure the extent of the attenuation at very low spatial frequencies.

Spatial frequency band widths for neurones in parafoveal V1 and V2 are shown in Fig. 4. The majority of cells in both cortical areas were classified as selective to spatial frequency, with most band widths ranging from 1 to 3 octaves. Of these, 8% of cells in V1 and 11% in V2 had band widths wider than 2·5 octaves. In V1 8% of cells and in V2 18% had band widths of 1·2 octaves or less and were thus narrowly tuned to spatial frequency. The *mean* band width of the bandpass cells was 1·8 octaves for parafoveal neurones in both V1 and V2. The ranges of band widths for simple and complex cells in the two cortical areas are similar (Fig. 4), but the low number of simple cells found precludes useful comparison of values for the means.

The optimum spatial frequencies for spatial-frequency-selective neurones in V1 and V2 are shown in Fig. 5. There is an approximately 4 octave range of preferred spatial frequencies in the two cortical areas. However, the sample in V1 is selective to a much higher range of spatial frequencies than is the sample in V2. There is, nevertheless, some overlap between the two distributions in the 0·7–2 cycles/deg range. The geometric mean for the V1 distribution was 2·2 cycles/deg, and the mean for the V2 population was 0·65 cycles/deg. The difference between the means was statistically significant ($t = 13{\cdot}3$, d.f. $= 211$, $P < 0{\cdot}001$). Thus, there is an approximately 3-fold difference in the mean of the optimum spatial frequency (as well as for the receptive field sizes) for cells in parafoveal V2 *versus* parafoveal V1.

The distribution of optimum spatial frequencies in V1 is unimodal, whereas the V2 distribution has a secondary peak at the bin labelled '$\leqslant 0{\cdot}25$ cycles/deg'. In several experiments we brought the cathode-ray tube close enough to the eye so that we could present spectrally compact gratings of extremely low spatial frequency and found neurones in parafoveal V2 with definite bandpass sensitivity selective to spatial frequencies as low as 0·25 cycles/deg.

In V1, optimum spatial frequencies for simple and complex cells covered essentially the same range and had approximately the same mean (Fig. 5*A*). However, in V2 the mean optimum spatial frequency for simple cells was 0·45 cycles/deg, which was lower than the mean of 0·79 cycles/deg for complex cells ($t = 2{\cdot}2$, d.f. $= 88$, $P < 0.05$). In V2, preferred spatial frequencies for both simple and complex cells were found in the range $< 0{\cdot}25$–0·7 cycles/deg, but only complex cells were found for spatial frequencies from 1·0 to 2·0 cycles/deg (Fig. 5*B*). Thus, there was only minimal overlap in the spatial frequency selectivities of simple cells in V1 and V2 compared to the broader overlap for the complex cell populations in the range 0·7–2·0 cycles/deg (Fig. 5).

Our *median* band width for neurones in macaque parafoveal V1 was 1·7 octaves. This estimate is slightly higher than the *median* of 1·5 octaves obtained from threshold measurements by DeValois *et al.* (1982), although there is general agreement in the range and distribution of band widths found in their study and our own. In addition, DeValois *et al.* (1982) found that the spatial frequency band widths of V1 neurones were negatively correlated with their optimum spatial frequencies. The mean spatial frequency band width for their V1 cells decreased by about 0·18 octaves

per octave increase in optimum spatial frequency. In our sample of V1 neurones, spatial frequency band widths decreased by 0·13 octaves per octave increase in optimum spatial frequency. The similarities in the range of optimum spatial frequencies, the range of band widths, and the decrease in band width with increasing optimum spatial frequency based upon threshold measures by DeValois *et al.* (1982), and the corresponding estimates based upon responsivity measurements in the

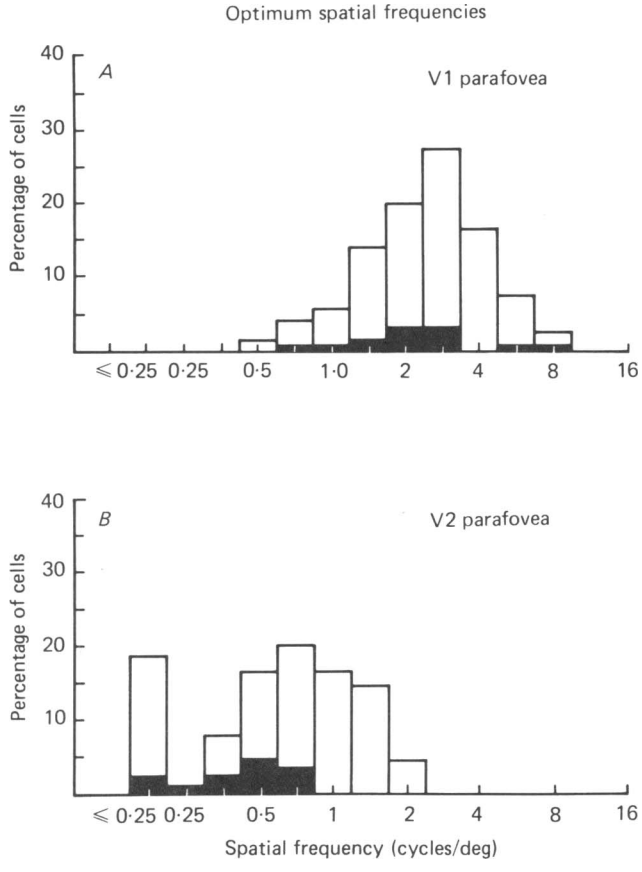

Fig. 5. The distribution of optimum spatial frequencies obtained from studies of parafoveal neurones is shown for V1 (*A*) and V2 (*B*). Those neurones which responded maximally at 0·25 cycles/deg and which for technical reasons were not tested below 0·25 cycles/deg are labelled ⩽ 0·25 cycles/deg. Simple cells are represented by the filled part of the bars, complex cells by the open part of the bars. The difference between the means of the distributions (V1 = 2·2 cycles/deg; V2 = 0·65 cycles/deg) is statistically significant. The overlap between the two distributions is principally in the 0·7–2 cycles/deg range.

present study, support the idea that the spatial frequency selectivity properties of neurones in V1 do not change much at suprathreshold contrast levels (Movshon *et al.* 1978*a*; Albrecht & Hamilton, 1982). There are no previous estimates of spatial frequency band widths for neurones in V2 of the macaque monkey.

Range and sequence of spatial frequency preferences within individual penetrations in V1 and V2. Most penetrations were made approximately normal to the cortical

laminae, and the receptive field centres shifted little within a penetration. Hence, the spread of spatial frequencies found within a penetration should sample the range found at a given retinal eccentricity. Within single penetrations in V1, spatial frequency preferences covered a span of 1·5–3·0 octaves. In parafoveal V2, a span of 3 octaves from 0·25 to 2·0 cycles/deg was commonly encountered.

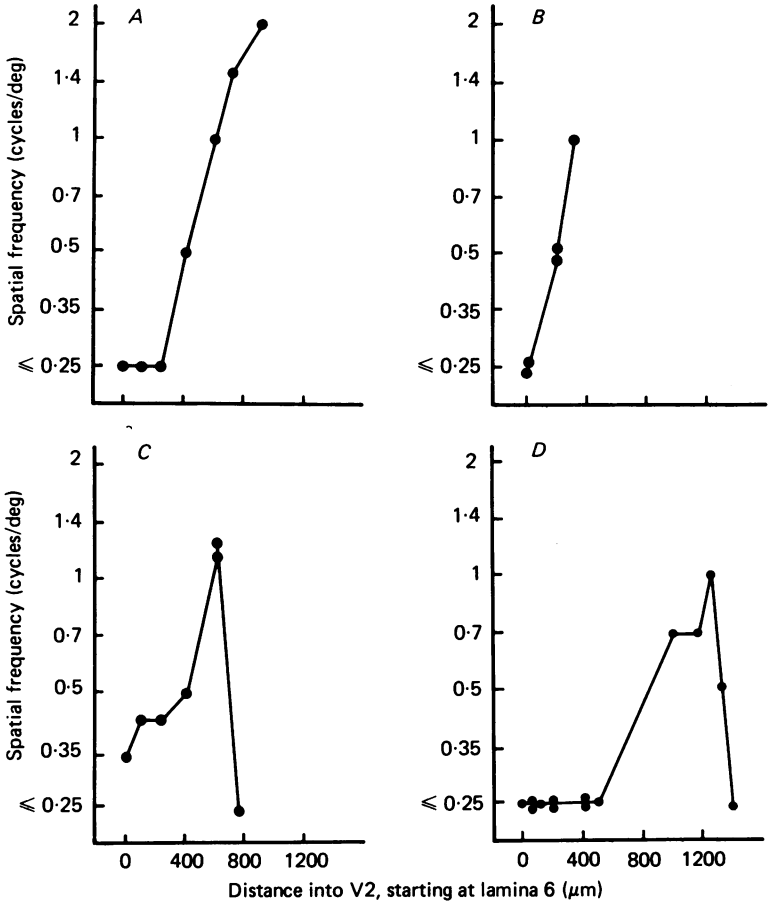

Fig. 6. Optimum spatial frequency is plotted as a function of distance into V2 for four penetrations in parafoveal V2. Because the electrode entered V2 from the underlying white matter, the first neurones encountered (distance = 0) were in lamina 6 in the infragranular layers and each subsequent neurone is closer to the supragranular layers. This pattern was found in six of eleven electrode penetrations which entered V2 approximately normal to lamina 6.

Because of the technical limitations associated with laminar localization which are discussed in the *Methods*, we were unable to provide a precise laminar localization for most cells. However, a striking sequence of changes in spatial frequency preference was found in six of eleven complete penetrations through V2. As the micro-electrode entered the infragranular layers from the underlying white matter, the first cell encountered was often tuned to an extremely low spatial frequency (usually

0·25 cycles/deg). With each successive advance of the micro-electrode, the spatial frequency preference typically either remained the same or increased in an orderly manner until preferred frequencies in the 2·0 cycles/deg range were found (Fig. 6). In some cases only an increase in preferred frequency was found (Fig. 6*A* and *B*). In other penetrations the last one or two cells encountered at the end of the penetration had preferences for low spatial frequencies (Fig. 6*C* and *D*). Although laminar localization along the full extent of the tract is uncertain, the results are sufficient to indicate that neurones with preferences for very low spatial frequencies are frequently found clustered within the infragranular layers.

In five of the eleven complete penetrations through V2, no such orderly sequence of preferred spatial frequencies was seen. Whether these discrepant results indicate an inhomogeneity in structural organization within V2 as suggested by metabolic studies (Tootell, Silverman, DeValois & Jacobs, 1983) or a sampling problem is unknown.

'*Complexity index*' *of neurones in V1 and V2*. Glezer *et al.* (1980) used the term 'complexity index' as a measure of the number of full cycles of the grating of optimum spatial frequency within the width of the receptive field of a complex cell. The index is simply the product of the preferred spatial frequency and the field width. The implication of 'complexity' arises from the suggestion that the number of cycles within the field may be proportional to the number of preceding subunits required to span the field width.

We calculated this index for neurones in V1 and V2 (Fig. 7). In both cortices the values were lower for simple cells than for complex cells. In both cortices the index most commonly ranged from 1·0 to 3·0, although some values up to 5·0 were found.

Occasionally, in both V1 and V2, neurones were found with indices less than 1·0, indicating that the receptive field width measured less than one full cycle of the sine-wave grating producing the strongest response. Such neurones comprised 8 % of the V1 parafoveal population and 23 % of the corresponding population in V2. The peak spatial frequency, band widths and responsivity to bars at the peak of the receptive field profile for these neurones spanned the same range as those for neurones with indices greater than 1·0. These results are difficult to understand unless the width of the field has been underestimated from the studies with single narrow drifting slits due to inadequate stimulation of receptive field fringes.

The spatial frequency band width was also plotted against the complexity index. For simple cells the band width narrowed with an increase in the index, decreasing from 2·1 octaves when the index was 1·0 to 1·24 octaves when the index was 3·0 (correlation coefficient = 0·56, $t = 3{\cdot}63$, d.f. = 26, $P < 0{\cdot}01$). For complex cells the band width failed to narrow with an increase index.

Temporal frequency selectivity. Examples of temporal frequency selectivity curves for three different neurones are shown in Fig. 8. In all curves, responses eventually fell off to zero (or sometimes even below the spontaneous level) when sufficiently high temporal frequencies were tested. Curves were considered as 'bandpass' when the responsivity dropped to well below 50 % of peak amplitude at temporal frequencies below as well as above the peak value at the optimum temporal frequency (Fig. 8*A*). In other curves, an optimum temporal frequency could be identified, but the fall-off on the low temporal frequency side was shallow, with response falling to only about

50 % of peak values for temporal frequencies as low as 0·5–0·7 Hz (Fig. 8*B*). In still other cells no definitely 'optimum' temporal frequency could be identified, and the responsivity at low temporal frequencies remained at high plateau level (Fig. 8*C*). Such curves indicate 'low-pass' temporal frequency selectivity. Individual curves retained their bandpass or low-pass temporal frequency characteristics independent of stimulus contrast. Furthermore, the type of temporal curve was not closely related

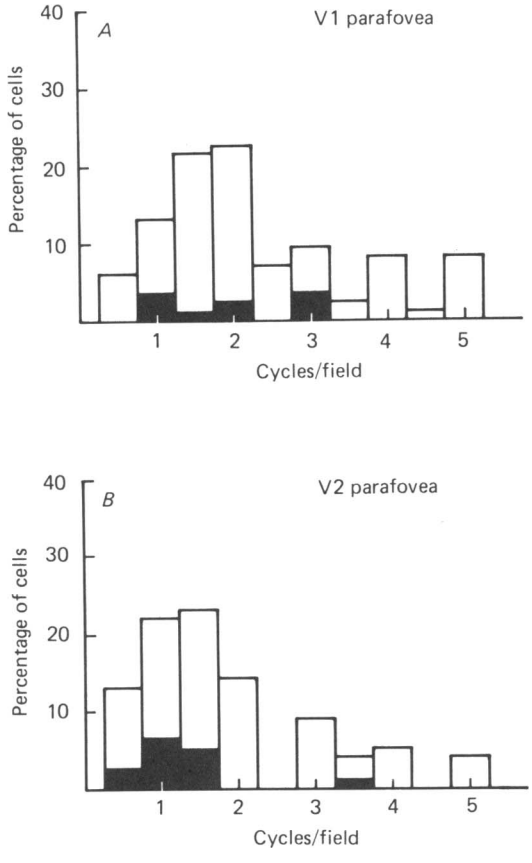

Fig. 7. The distribution of the number of cycles of the sine-wave grating of the optimum spatial frequency which can be fitted within the neurone's receptive field is shown for V1 (*A*) and V2 (*B*). Simple cells are represented by the filled part of the bars, complex cells by the open part.

to neuronal responsivity under anaesthesia, inasmuch as in several dual recording situations one neurone had pronounced bandpass selectivity whereas the other cell had low-pass temporal selectivity.

Although all three types of curves were found for neurones in V1 and V2, there were major differences in the incidence of the type of temporal frequency selectivity curves found in the two cortices. In V1 68 % of the parafoveal neurones showed either flat low-pass or shallow low-pass temporal frequency selectivity (Fig. 9*A*), whereas in parafoveal V2 only 36 % of neurones showed either flat or shallow low-pass

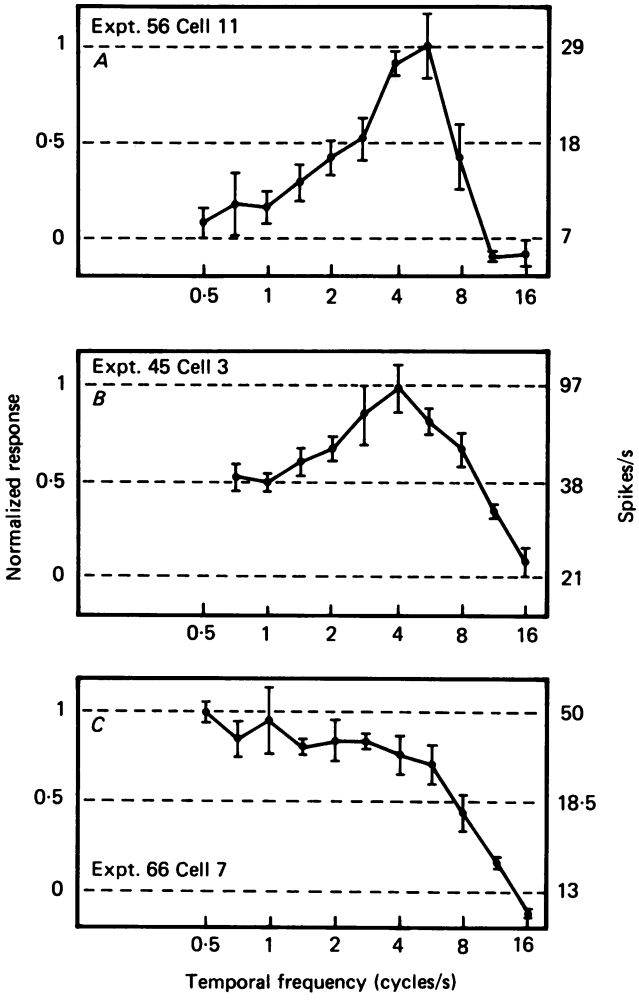

Fig. 8. Temporal frequency tuning curves obtained from three neurones shown to illustrate the types of curves found in this study: first, those which respond to only a limited range of the temporal frequency spectrum (*A*); secondly, those with a defineable peak frequency but with only modest low frequency attenuation (*B*); thirdly, those having no identifiable peak frequency because of little or no low frequency attenuation (*C*). For each curve the maximum response has been normalized to 1 on the left side of the vertical axis, with 0·0 corresponding to the spontaneous firing rate. The right side of the vertical axis is scaled in spikes/s.

selectivity (Fig. 9*B*). (In both V1 and V2, clear examples of both low-pass and bandpass temporal selectivity were found for both simple and complex cells, and the distributions of band widths were spread over a wide range for both cell types (Fig. 9).) Not only did the percentage of parafoveal neurones with bandpass temporal frequency selectivity increase from 32 to 64 % from V1 to V2 ($\chi^2 = 17{\cdot}36$, d.f. = 1, $P < 0{\cdot}001$), but the mean band widths for those tuning curves classified as 'selective' narrowed from 2·9 octaves in V1 to 2·1 octaves in V2 ($t = 4{\cdot}60$, d.f. = 77, $P < 0{\cdot}001$).

Further, when considering all temporal frequency selectivity curves, the differences between V1 and V2 become more striking. In V1 only 15 % of neurones had temporal frequency band widths below 2·75 octaves, whereas in V2 the majority of neurones (54 %) had such band widths (Fig. 9).

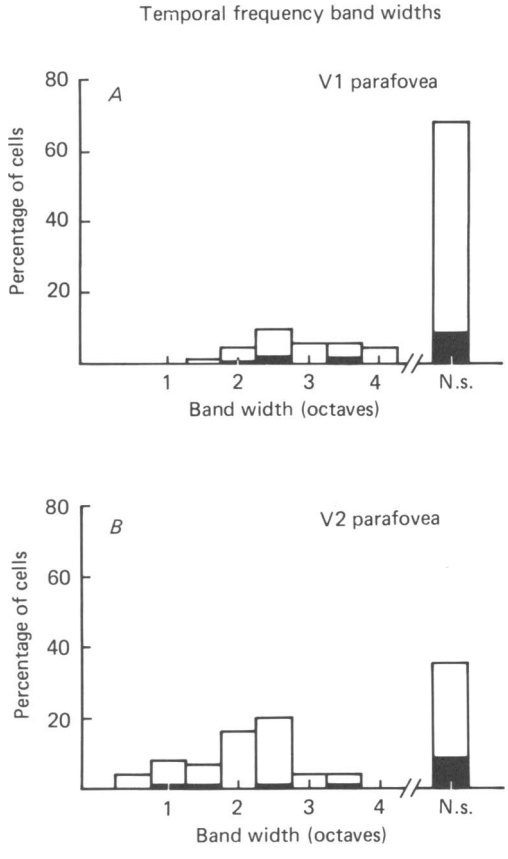

Fig. 9. The distributions of temporal frequency band widths obtained from studies of parafoveal neurones are shown for V1 (*A*) and V2 (*B*). Simple cells are represented by the filled part of the bars, complex cells by the open part of the bars. Those neurones classified as non-selective for temporal frequency (see examples in Fig. 8 *B* and *C*) are labelled as N.s. Note that V1 has a larger percentage of such non-selective neurones than does V2.

On the other hand, the range and distribution of optimum temporal frequencies were very similar in V1 and V2 (Fig. 10), with the average optimum temporal frequency being 3·7 Hz in V1 and 3·5 Hz in V2.

When 50 % cut-offs at high temporal frequencies are considered, some distinctions emerge between neurones in the two cortical areas (Fig. 11). In V1, most high frequency cut-offs range from 5·6 to 16·0 Hz (Fig. 11 *A*). In V2, this range is also well represented; however, there is a greater percentage of neurones with high frequency cut-offs in the lower ranges of temporal frequency (Fig. 11 *B*). This latter result probably reflects the greater tendency for neurones in V2 to have greater temporal

frequency selectivity and for the peak values to be dispersed across the temporal frequency spectrum. In the two cortices, simple cells seem to share the same range of high frequency cut-offs as complex cells (Fig. 11). In V2, the number of cells increases as a function of the high 50 % cut-off from 1 to 11·3 Hz (Fig. 11*B*).

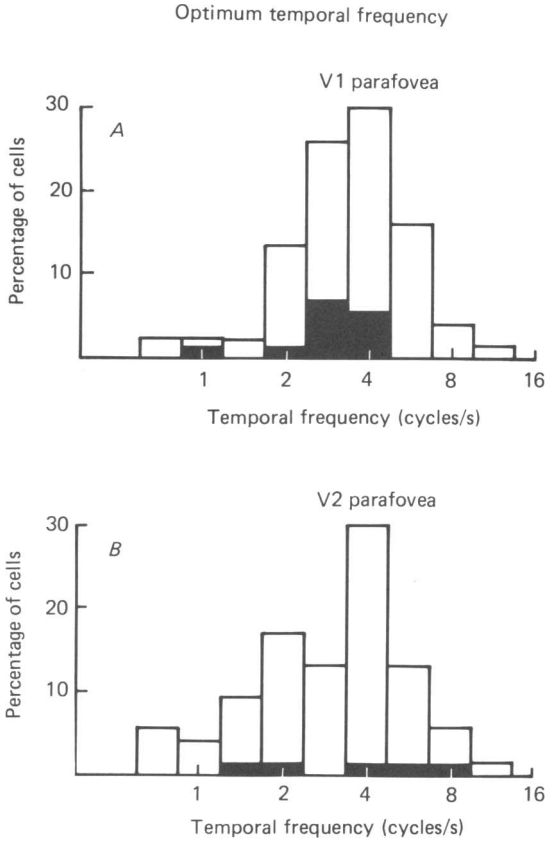

Fig. 10. The distributions of optimum temporal frequencies obtained from studies of parafoveal neurones are shown for V1 (*A*) and V2 (*B*). Simple cells are represented by the filled part of the bars, complex cells by the open part of the bars. In addition to data from bandpass cells (Fig. 8*A*), the Figure includes data from neurones which had a discernible peak but with insufficient low-frequency attenuation to be classified as bandpass (Fig. 8*B*.)

The temporal frequency at which the high frequency side of the temporal frequency tuning curve intersected the spontaneous firing level was taken as a measure of the temporal frequency resolution of a cell. On average, the resolution was about 0·8 octave above a cells's high 50 % cut-off. The highest values of temporal frequency resolution (30–40 cycles/s) were similar for V1 and V2. The psychophysically measured temporal frequency resolution of the human visual system is also about 30–40 cycles/s for 2·5 deg by 2·5 deg sine-wave grating patches for spatial frequencies of 0·5 and cycles/deg at contrasts of 0·3–0·4 (Robson, 1966). However, when larger grating patches (16 deg by 8 deg) are used, the temporal frequency resolution of the human visual system is over 50 cycles/s at 30 % contrast (Kelly, 1969).

We found no statistically significant relationship between optimum temporal frequency and temporal frequency band width. Thus, unlike the results for spatial frequency band widths which narrowed at high optimum spatial frequencies, there was no evidence for a narrowing of temporal frequency band width at higher temporal frequencies.

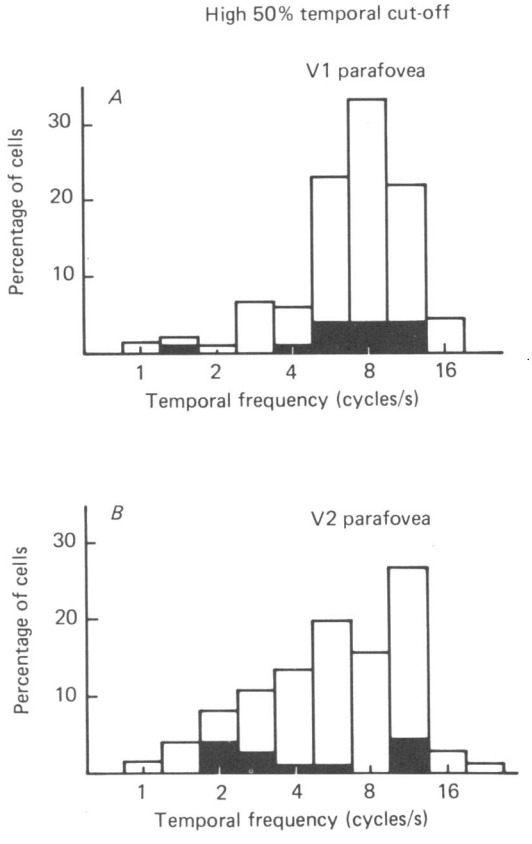

Fig. 11. The distributions of the temporal high frequency 50% cut-off obtained from studies of parafoveal neurones is shown for V1 (*A*) and V2 (*B*). This Figure allows the comparison of the temporal frequency resolution of all neurones including those non-selective neurones for which an optimum temporal frequency could not be found. Note that the two distributions cover the same range but the shapes of the distributions are different.

Studies of the temporal frequency selectivity of neurones in area 17 and 18 of the cat (Berardi *et al.* 1982) have emphasized the higher calculated preferred drift velocities for neurones in area 18 compared to 17. In our macaque data, a similar calculation could be made, but the higher drift velocities for V2 would essentially reflect the much lower spatial frequency preferences of these neurones, while resolution for temporal frequency is much more similar in the two cortices.

Spatio-temporal tuning surfaces in V1 and V2. Spatial frequency selectivity curves were measured at a constant temporal frequency, and temporal frequency tuning

curves were measured at a constant spatial frequency. The one-dimensional tuning curves presented above are not sufficient to determine whether the cells were independently selective to the spatial frequency of the grating, the temporal frequency of the grating, or to what extent there is an interaction between the spatial and temporal frequency variables. We investigated this issue by measuring tuning surfaces in which the response was measured to a set of gratings whose spatial and temporal frequencies formed a grid of points in the spatio-temporal frequency plane.

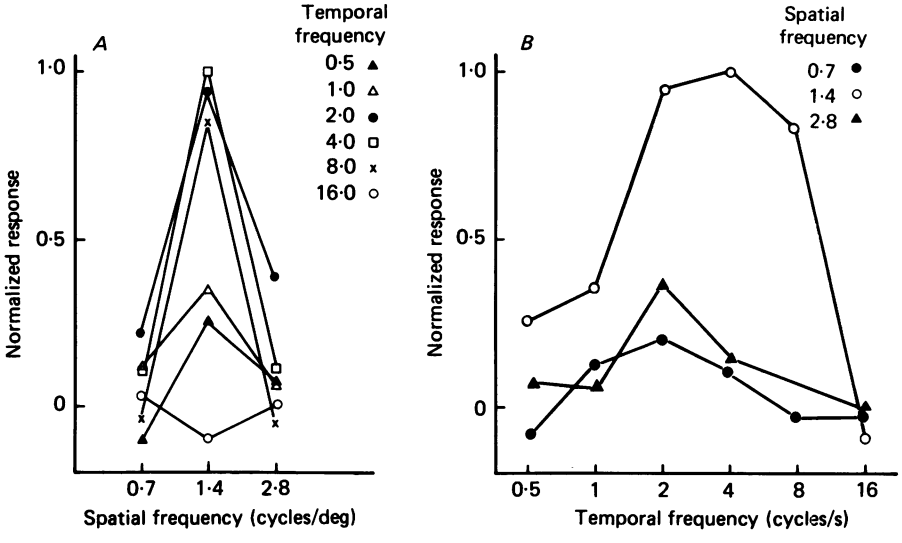

Fig. 12. *A* is a plot of a set of spatial frequency tuning curves obtained from a neurone in V2. Each curve was measured at a different temporal frequency as shown by the symbol legend. For temporal frequencies between 0·5 and 8 cycles/s, the maximum response of each spatial frequency tuning curve occurred at 1·4 cycles/deg. *B* shows the same data plotted as temporal frequency tuning curves measured using different spatial frequency gratings. The peaks of the temporal frequency tuning curves measured using 0·7 and 2·8 cycles/deg gratings occur at a lower temporal frequency than the peak of the temporal frequency tuning curve measured at the optimum spatial frequency.

We carried out detailed measurements of the spatio-temporal tuning surface of two neurones in V1 with broad bandpass temporal frequency selectivity and also sequentially measured spatial frequency tuning curves, using different temporal frequencies for two additional cells in V1 with low-pass temporal frequency selectivity. No systematic changes in tuning properties were found, a result consistent with similar studies in V1 of the cat (Tolhurst & Movshon, 1975; Holub & Morton-Gibson, 1981). We then directed particular attention to the spatio-temporal surfaces of V2 cells, because they were more likely to be substantially band-limited in both the spatial and temporal frequency domains.

The results from a V2 cell are shown in Fig. 12. The left panel shows a plot of a set of spatial frequency tuning curves obtained by 'slicing' the tuning surface orthogonal to the temporal frequency axis. Each curve is a spatial frequency tuning curve measured at a given temporal frequency which is different for each curve. For

temporal frequencies between 0·5 and 8 cycles/s, the maximum response of each spatial frequency tuning curve occurred at 1·4 cycles/deg.

The right panel of Fig. 12 shows the same data plotted as temporal frequency tuning curves measured using different spatial frequencies. The peaks of the temporal frequency tuning curves measured using 0·7 and 2·8 cycles/deg gratings are lower in amplitude than the peak of the temporal frequency tuning curve obtained using the optimum spatial frequency of 1·4 cycles/deg. Moreover, the peaks of the temporal frequency curves tested at non-optimum spatial frequencies shifted towards slightly lower values of temporal frequency (Fig. 12*B*).

We quantitativity evaluated the extent of spatio-temporal interaction from the data points comprising each spatio-temporal surface. The peak values for each tuning curve were first estimated using a cubic spline interpolation. The average shifts in peak value along both the spatial and temporal frequency axes were then calculated for eight cells in V2 (Fig. 13). The origin of the graph represents 'zero shift', i.e. the point representing the preferred spatial and temporal frequency for each cell. The data points represent the average shift in the peaks of the tuning curves (± 2 S.E. of mean) when measured at non-optimum frequencies. The data points with vertical error bars represent the average shifts in preferred spatial frequency when measured at temporal frequencies 1 and 2 octaves above and below the preferred temporal frequency. The data points with horizontal error bars represent the average shift in preferred temporal frequency when measured at spatial frequencies 1 octave above and below the preferred spatial frequency. (Note that the only tuning curves which had peaks which were at least 10 % of the maximum response were measured. Thus, tuning curves with low response magnitudes were excluded.)

If the variables of spatial frequency and temporal frequency were entirely separable, then the data points should have fallen on the X or Y axis. If, however, the cell were tuned to the velocity of the grating, then the data points should have fallen along the diagonal line in Fig. 13. The data are not consistent with the prediction of velocity tuning.

The average shift of the spatial frequency tuning curve peak is not significantly different from zero, indicating that the peak of the spatial frequency tuning curve does not depend on the temporal frequency. When the temporal frequency tuning curves were measured using a spatial frequency which was 1 octave below the optimum spatial frequency, the average shift in the peak of the temporal frequency tuning curves was only $-0{\cdot}21$ octave. When the temporal frequency tuning curves were measured at 1 octave above the preferred spatial frequency the average shift in the peak of the temporal frequency tuning curves was $-0{\cdot}36$ octave. Both of these shifts were statistically significant at the 0·05 level. Thus, the temporal frequency response curves shift to slightly lower temporal frequencies when measured using a grating of non-optimum spatial frequency. The shifts in the optima of the temporal frequency tuning curves rule out the possibility that the spatio-temporal surface can be described by the product of a spatial frequency tuning function and a temporal frequency tuning function. Thus, the spatio-temporal tuning surface is not strictly separable.

We also compared the band widths of spatial frequency tuning curves measured using non-optimum temporal frequencies with spatial frequency tuning curves

measured using optimum temporal frequencies. No statistically significant trends were found. It should be stressed, however, that the 1 octave sampling interval of the stimulus and the generally low response density of cells stimulated at non-optimum temporal frequencies, make a precise estimate of band width difficult under these conditions. However, the measurements were sufficient for detection of any large changes in the shapes of tuning curves, and we found no evidence that cells which exhibited bandpass spatial frequency tuning when measured at optimum temporal

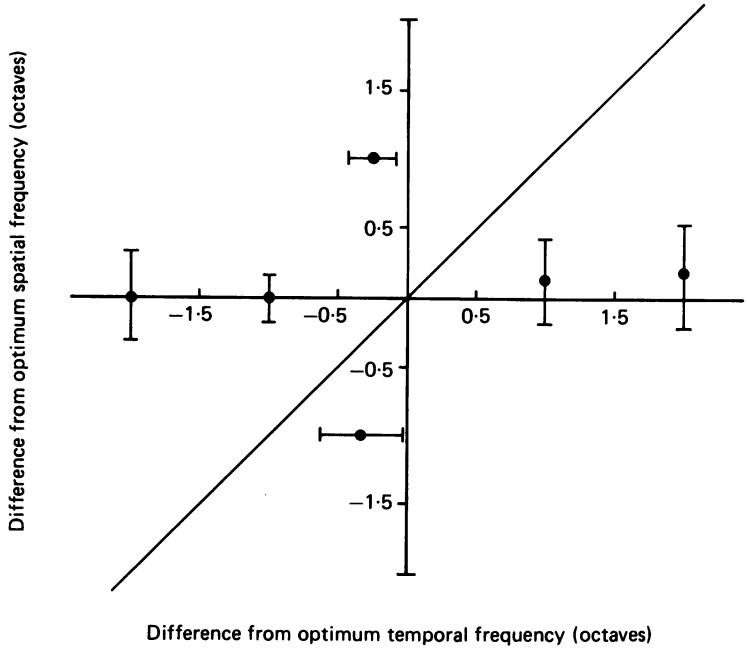

Fig. 13. The peak shifts of tuning curves measured at non-optimum frequencies are summarized from spatio-temporal tuning surfaces obtained from eight neurones in V2. The data points represent the average shift in the peaks of the tuning curves (±2 S.E. of mean) when measured at non-optimum frequencies. For data relating to spatial frequency tuning curves (vertical error bars), the *X* axis represents the difference, in octaves, between the optimum temporal frequency and the temporal frequency at which the spatial frequency tuning curve was measured, and the *Y* axis represents the peak shift, in octaves, relative to the optimum spatial frequency. For data related to temporal frequency tuning curves (horizontal error bars) the *X* axis represents the peak shift, in octaves, of the temporal frequency tuning curve relative to the optimum temporal frequency, and the *Y* axis represents the difference, in octaves, between the optimum spatial frequency and the spatial frequency at which the temporal frequency curve was measured.

frequencies exhibited low-pass spatial frequency tuning when stimulated at non-optimum temporal frequencies (Fig. 12*A*). Similarly, cells which exhibited bandpass temporal selectivity when tested at the preferred spatial frequency continued to show bandpass temporal tuning when tested at non-optimum spatial frequencies (Fig. 12*B*).

We also made sequential measurements of pairs of spatial frequency tuning curves using different temporal frequencies for another seven cells in V2. Again we found

no evidence to suggest that the optimum spatial frequency or general shape of the tuning curve changed when tested at a non-optimum temporal frequency.

To summarize, although our results in V2 show that the spatio-temporal tuning surfaces of these cells are not perfectly separable into spatial and temporal functions,

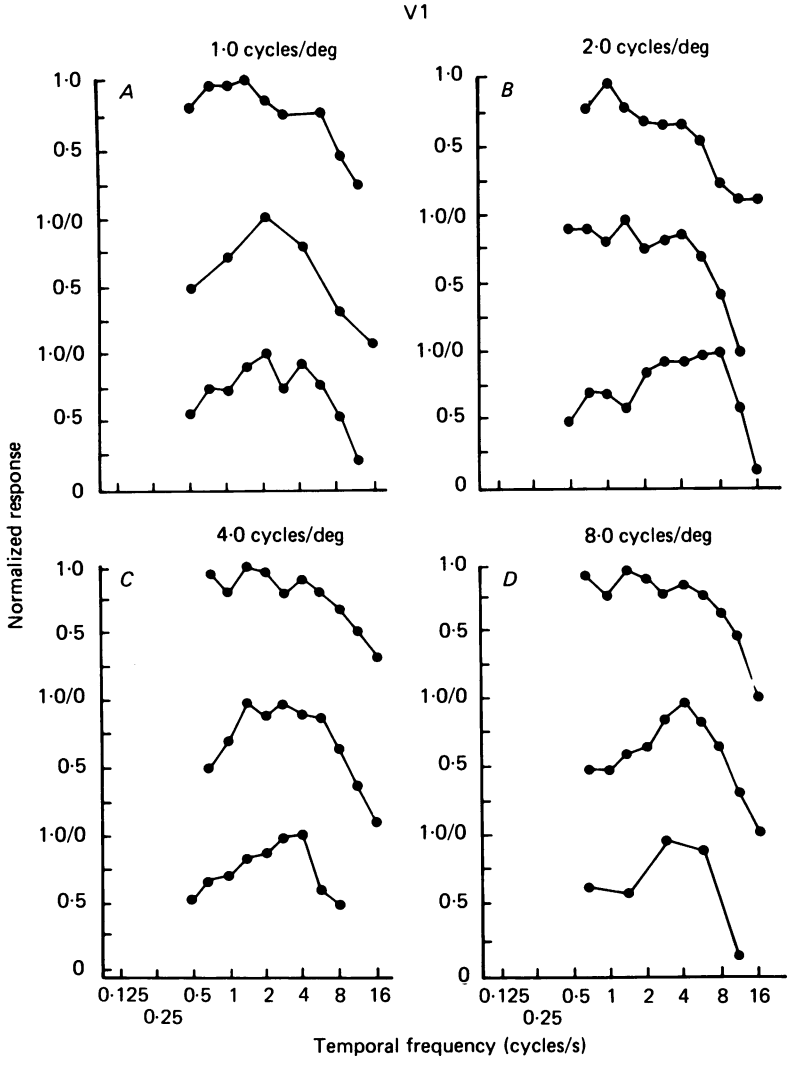

Fig. 14. Temporal frequency tuning curves are shown for neurones in parafoveal V1 which had the same optimum spatial frequency of either 1 cycle/deg (*A*), 2 cycles/deg (*B*), 4 cycles/deg (*C*), or 8 cycles/deg (*D*). For each curve, the maximal response has been normalized to 1·0 on the vertical axis, with 0·0 representing the spontaneous firing rate.

we found no evidence for a strong interaction in either V1 or V2 cells. Thus those V2 cells which are most often band-limited for both spatial frequency and temporal frequency respond well to stimulation within only a restricted region of the two-dimensional spatio-temporal frequency plane.

There are at present no other results on this issue in either V1 or V2 in the macaque

monkey. Our results are essentially similar to those in area 17 of the cat found by Ikeda & Wright (1975), Tolhurst & Movshon (1975) and Holub & Morton-Gibson (1981). However, Bisti, Carmignoto, Galli & Maffei (1984) have reported that peak spatial frequencies of neurones in area 18 of the cat shift towards lower values (though

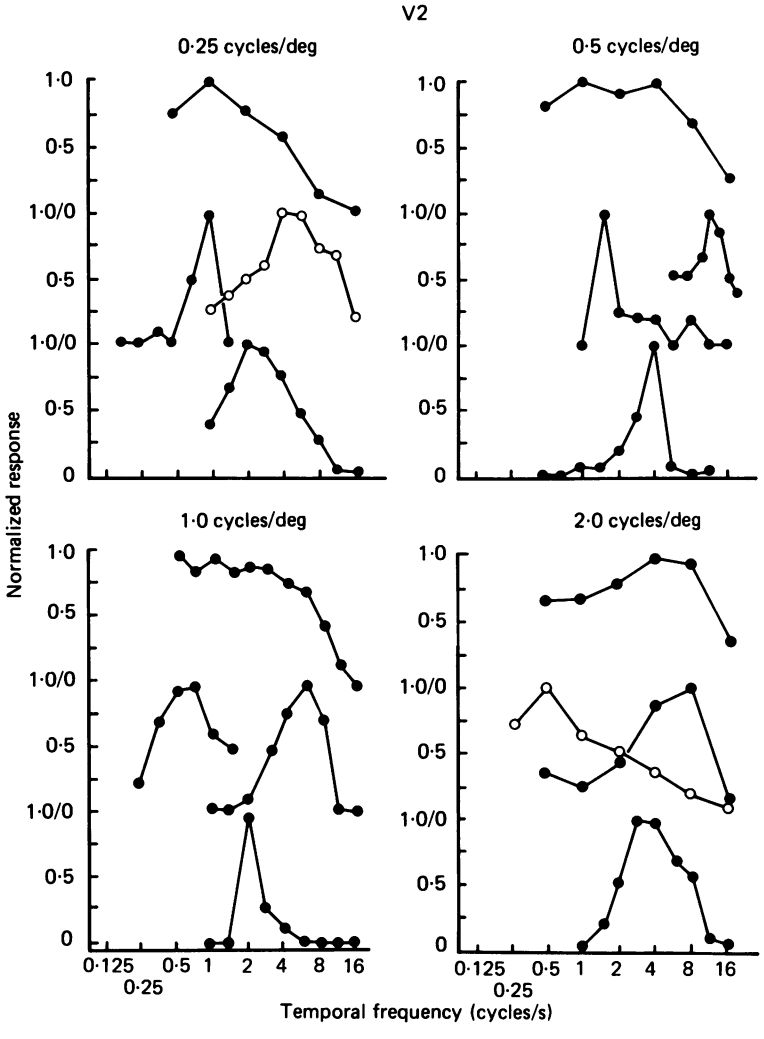

Fig. 15. Temporal frequency tuning curves are shown for neurones in parafoveal V2 which had the same optimum spatial frequency of either 0·25 cycles/deg (*A*), 0·5 cycles/deg (*B*), 1·0 cycles/deg (*C*), or 2·0 cycles/deg (*C*). For each curve, the maximal response has been normalized to 1·0 on the vertical axis, with 0·0 representing the spontaneous firing rate.

not inversely so) at increasing drift velocities yet with little change in peak responsiveness. Therefore, cells in area 18 of the cat respond to a much larger area of the spatio-temporal frequency plane than do cells in V2 of the macaque monkey.

In man there is psychophysical evidence that contrast sensitivity at low spatial frequencies of the *entire* visual system increases at higher velocities (Burr & Ross,

1982). However, psychophysical studies of individual transient mechanisms in human vision suggest spatio-temporal separability (Wilson, 1980), a result which is closer to the findings in V2 of the macaque monkey than to those in area 18 of the cat.

Relationship between spatial and temporal frequency selectivity at the population level. The optimum spatial frequency and optimum temporal frequency were not correlated in either the parafoveal V1 or parafoveal V2 samples. The same result has been reported in comparable studies in the cat (Ikeda & Wright, 1975; Holub & Morton-Gibson, 1981). When data from V1 and V2 were examined separately we found no relationship between the optimum spatial frequency of a cell and the type of temporal frequency selectivity. That is, examples of cells with either low-pass or bandpass temporal frequency selectivity were found over the respective ranges of spatial frequencies represented in V1 (Fig. 14) and V2 (Fig. 15). However, it must be re-emphasized that the majority of neurones in V1 had low-pass temporal frequency selectivity, where those neurones in V1 with bandpass temporal selectivity generally had very broad band widths (Fig. 14). Thus, for each preferred spatial frequency in V1, there exists a minimum of two temporal-frequency-selective mechanisms, one with low-pass selectivity, the other with broadly tuned bandpass selectivity (Fig. 14). The broadly tuned temporal curves in V1 overlap each other substantially (Fig. 14).

On the other hand, the results in V2 suggest that for each preferred spatial frequency there exists a minimum of three temporal-frequency-selective mechanisms. At each spatial frequency, some examples of curves with low-pass temporal frequency selectively are found, but additionally there is evidence for a minimum of two bandpass temporal-frequency-selective mechanisms spaced with minimal overlap across the temporal frequency spectrum (Fig. 15).

Spatial and temporal frequency-specific inhibition of neurones in V1 and V2

Inhibition of spontaneous activity. In order to determine whether spatial or temporal frequencies outside the excitatory bandpass of the cell inhibit neuronal activity, it is necessary to have a spontaneous level of activity sufficiently high to evaluate inhibitory effects. This requirement was met for seventy-nine neurones in V1 and eighty-five neurones in V2.

Within this subpopulation, inhibitory responses were found for certain extended gratings which covered both the classically defined receptive field as mapped by single slit studies (Hubel & Wiesel, 1968) and the 'unresponsive regions' surrounding the classical field (Maffei & Fiorentini, 1976). Twenty-six of the seventy-nine cell subset in V1 and twenty-one of the eighty-five cell subset in V2 showed significant reduction ($P < 0{\cdot}001$) of the spontaneous activity at one or more spatial frequencies. The spatial frequencies producing such inhibition were significantly more likely to be higher than the peak excitatory frequency (f) than lower ($\chi^2 = 8{\cdot}9$, d.f. $= 1$, $P < 0{\cdot}01$). This result is analogous to the finding reported by DeValois & Tootell (1983) for neurones in area 17 of the cat. The spatial frequencies producing maximal inhibition were most commonly in the range of 3–5f in both V1 and V2. Thus, just as the optimum spatial frequencies for excitation were much lower in V2 than in V1, so the range of frequencies producing inhibition in V2 was correspondingly lower than in V1.

A small subset of neurones (seven of seventy-nine in V1 and eight of eighty-five

in V2) showed inhibition of spontaneous activity at certain temporal frequencies. The temporal frequencies producing inhibition were higher than the optimum temporal frequencies more often than they were lower ($\chi^2 = 13{\cdot}6$, d.f. $= 1$, $P < 0{\cdot}001$). The cells exhibiting such inhibition were significantly more likely to have temporal bandpass than low-pass characteristics ($\chi^2 = 7{\cdot}0$, d.f. $= 1$, $P < 0{\cdot}01$). Furthermore, the band-pass cells showing inhibition had significantly narrower temporal frequency band widths than those not showing inhibition ($t = 2{\cdot}61$, d.f. $= 67$, $P < 0{\cdot}02$).

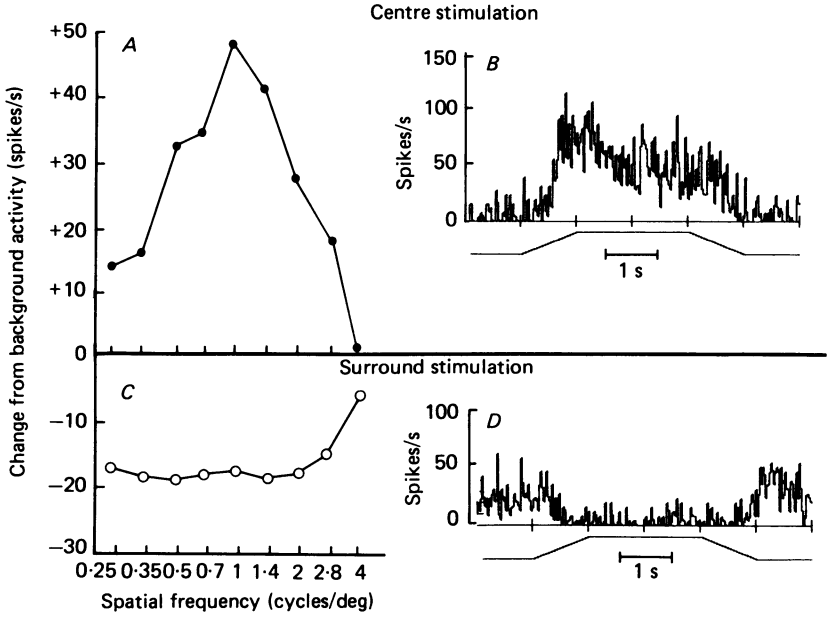

Fig. 16. The spatial frequency selectivity curve obtained when the sine-wave grating was restricted to the classical receptive field, as mapped by a single slit, is shown in *A*. The histogram of the excitatory response to the optimum grating 1 cycle/deg) is shown in *B*. The spatial frequency selectivity curve of the 'unresponsive regions' was obtained by continuously drifting a grating of 1 cycle/deg in the classical field while presenting our normal interleaved series of gratings in a region extending well beyond the classical field (*C*). The histogram of the inhibitory response when a grating of 0·7 cycles/deg is presented in the surround is shown in *D*.

Inhibition of evoked activity. We studied seven neurones in parafoveal V2 to determine whether there were inhibitory effects on the activity evoked by stimulation of the classical receptive field by simultaneous stimulation of the 'unresponsive regions' extending beyond the classical field. We initiated these studies after finding that the use of an extended grating resulted in a profound inhibition of neuronal activity. In all seven cases, gratings limited by a circular aperture to the classical field produced a strong excitatory response (Fig. 16*B*), whereas simultaneous presentation of a second grating filling the 10 deg by 12 deg scope face outside the aperture produced inhibitory effects (Fig. 16*D*). For five cells, maximal inhibition was produced by the spatial frequency that maximally excited the classical receptive

field. The remaining two cells exhibited an inhibitory response to a broad range of spatial frequencies ($\sim$ 4 octaves), and thus the inhibitory curves for the 'unresponsive regions' (Fig. 16*C*) were much more broadly tuned for spatial frequency than was the excitatory curve for the classical field (Fig. 16*A*).

In three of the seven cases, the cut-off for spatial frequencies producing an inhibitory response in the 'unresponsive regions' was an octave higher than the cut-off for producing an excitatory response in the classical field. However, the high cut-off for spatial frequencies producing inhibitory responses in parafoveal V2 never exceeded 4·0 cycles/deg, which is the same value for the high cut-off frequency that produced excitatory responses in parafoveal V2. This result suggests that neurones in parafoveal V2 respond to only the lower and middle ranges of spatial frequencies whether the stimulus produces excitation or inhibition.

Comparison of foveal and parafoveal neurones in V1 and V2

We studied eighteen neurones in V1 and twenty-six neurones in V2 at a retinal eccentricity of 0·5–1·0 deg so that we could make some comparison of foveal neurones with those of our much larger parafoveal populations (Table 1).

Foveal V2 cells, when compared to foveal V1 cells, had lower optimum spatial frequencies, larger receptive field widths and were more likely to exhibit bandpass temporal frequency selectivity. That is, response properties which differed between neurones in V1 and V2 in the parafoveal samples also differed between V1 and V2 in the foveal samples.

Gattass *et al.* (1981) have shown that receptive field size increases with eccentricity at a faster rate in V2 than in V1. Therefore, the difference between the average receptive field size of V1 and V2 cells at a common eccentricity becomes larger as eccentricity is increased. Our data are consistent with this finding. Whereas the average receptive field width of foveal V2 cells was about 2 times larger than that of foveal V1 cells, fields of parafoveal V2 cells were about 3 times larger than those of parafoveal V1 cells. In addition, the present results suggest that optimum spatial frequency may decrease with eccentricity at a faster rate in V2 than it does in V1. Whereas the average optimum spatial frequency of foveal V2 cells was about half that of foveal V1 cells, the average optimum spatial frequencies of parafoveal V1 cells was about a third that of parafoveal cells. Thus at the two eccentricities examined, the ratio of average receptive field size to average optimum spatial frequency remains approximately constant.

Directional sensitivity. If the response in one direction was at least twice that in the opposite direction, then the cell was classified as directionally sensitive. 20% of our V1 cells (22 of 108) were directionally sensitive, lower than the 49% value reported by Schiller *et al.* (1976*b*) but similar to the 29% value reported by DeValois *et al.* (1982). In our study, V2 had a significantly greater percentage of directionally sensitive cells (V2 = 38%; 38 of 99) than did V1 ($\chi^2 = 4{\cdot}07$, d.f. = 1, $P < 0{\cdot}05$).

Because the V2 population represented a lower band of spatial frequencies than the V1 population, the results also indicate that the percentage of directionally selective cells is greater in the population preferring low spatial frequencies. Furthermore, within each cortical area there is an increased percentage of directionally sensitive cells at low spatial frequencies. There was no consistent relationship between

the percentage of directional selectivity and the temporal frequency high 50 % cut-off when this variable was considered independently of the spatial frequency.

The lowest percentage of directionally sensitive cells is found within the high spatial frequency–low temporal frequency subgroup of V1, and the highest percentage of directionally sensitive cells is found within the low spatial frequency–high temporal frequency subgroup of V2. These two subgroups represent the lowest and highest velocities, respectively, in the V1 and V2 population (Table 2). Thus, cells preferring higher velocities tended more often to be directionally selective.

TABLE 1. Spatial and temporal frequency characteristics and receptive field widths of neurones in the foveal and parafoveal regions of V1 and V2

Measurement		Parafovea	Fovea
Total cells	V1	130	18
	V2	96	26
Spatial frequency selective (%)	V1	91	88
	V2	100	100
Mean spatial frequency band width (octaves)	V1	1·8	1·4
	V2	1·8	1·6
Mean optimum spatial frequency (cycles/deg)	V1	2·2	4·2
	V2	0·65	2·7
Mean receptive field width (deg)	V1	1·1	0·4
	V2	3·0	0·9
Temporal frequency selective (%)	V1	32	33
	V2	64	92
Mean temporal frequency band width of selective cells (octaves)	V1	2·9	3·2
	V2	2·1	2·2
Mean optimum temporal frequency (cycles/s)	V1	3·7	4·4
	V2	3·5	4·7

TABLE 2. Percentage of neurones in V1 and V2 exhibiting directional selectivity as a function of cortical area and optimum spatial frequency

Cortical area	Optimum spatial frequency (cycles/deg)	Temporal frequency high 50 % cut-off (cycles/s)	Cells exhibiting directional selectivity (%)
V1	> 2·3	< 8·0	10
		⩾ 8·0	15
	⩽ 2·3	< 8·0	27
		⩾ 8·0	25
V2	> 0·6	< 8·0	33
		⩾ 8·0	22
	⩽ 0·6	< 8·0	41
		⩾ 8·0	57

Finally, in the V2 cell sample, directionally sensitive cells were more often bandpass temporally than were the directionally insensitive cells. Whereas 87 % of directionally sensitive cells had bandpass temporal frequency selectivity, only 57 % of directionally insensitive cells had bandpass temporal selectivity. This difference was statistically significant ($\chi^2 = 6{\cdot}25$, d.f. $= 1$, $P < 0{\cdot}05$).

DISCUSSION

Spatial frequency selectivity of neurones in V1 and V2

Selectivity of neurones in V1. The range of preferred spatial frequencies in parafoveal V1 was 0·5–8·0 cycles/deg, similar to the range found by Schiller *et al.* (1976*a*) and DeValois *et al.* (1982). The most common preferred spatial frequency was 2·8 cycles/deg, with the incidence dropping sharply with successively higher spatial frequencies of 4·0, 5·6 and 8·0 cycles/deg. This sharp decrease in the incidence of neurones preferring high spatial frequencies was also found in the two previously cited studies. This decreased incidence in the percentage of neurones representing the highest spatial frequencies is also seen in results on foveal neurones. The percentage of cells in the range of 8–16 cycles/deg was very low in the large foveal sample of DeValois *et al.* (1982) and in our smaller foveal sample.

A decreased incidence of neurones preferring higher spatial frequency may seem a surprising result. If receptive field widths at any given retinal eccentricity were independent of the preferred spatial frequency, and if the relative (octave) band width narrowed with increase in spatial frequency, then an efficient sampling model would predict an equal number of spatial frequency-selective neurones uniformally distributed across the spectrum. However, in our study and that of Schiller *et al.* (1976*a*), receptive field widths decrease with increasing preferred spatial frequency. Moreover, although there is some reduction of relative band width with increasing spatial frequency, this difference over the 3 octave range from 1·0 to 8·0 cycles/deg is only 0·4 octaves in our work and 0·55 octaves in the study of DeValois *et al.* (1982). This decrease in band widths is much too small to support a model of fixed receptive field widths with coherent linear summation. On the other hand, if field widths decrease with increasing preferred spatial frequency, then considerations of sampling theory suggest that there should be an even greater increase in the number of cells with increasing spatial frequency (Sakitt & Barlow, 1982). However, we cannot exclude the possibility that certain bands of spatial frequency, in this case the middle spatial frequencies, are oversampled (Kulikowski, Marcelja & Bishop, 1982) and/or contribute to diverse functional subsystems (S. Marcelja, personal communication).

Selectivity of neurones in V2. Our results on the spatial frequency selectivity of neurones in V2 permit comparisons with corresponding properties in V1. The major difference is that the V2 population samples a lower range of spatial frequencies extending from 0·25–2·0 cycles/deg in the parafovea to 0·5–5·6 cycles/deg in the fovea. In the parafoveal distribution, preferred spatial frequencies overlap primarily in the 1·0–2·0 cycles/deg range; the distributions are otherwise non-overlapping. We considered the possibility that our failure to find neurones in V2 with preferences for higher spatial frequencies reflected a sampling bias. However, a comparison of the highest spatial frequencies producing either excitation of the classical receptive fields or inhibition from receptive field 'non-responsive regions' revealed the same high 50 % cut-off frequency of about 2·8 cycles/deg. Even the very broadly tuned inhibition from the 'non-responsive regions' which was of equal magnitude over a 3 octave range up to 2·0 cycles/deg fell off to half-amplitude between 2·8 and 4·0 cycles/deg. Consequently, it may be that the higher ranges of spatial frequency are not represented in V2.

Comparisons between neurones in V1 and V2. On the other hand, there are a number of similarities between the two cortices. In both areas, the range of preferred spatial frequencies encountered within a single penetration may span a 3 octave range. The spatial frequency band widths in the two cortical areas are similar, with a mean value of 1·8 octaves for neurones in the two parafoveal populations, and a mean value of 1·4 octaves and 1·6 octaves respectively for neurones in the fovea of V1 and V2. The two cortices are also similar with respect to functional cell types, with simple as well as complex cells being present in both. The larger receptive field widths of neurones in V2 compared to widths in V1 seems largely associated with the lower range of spatial frequencies in V2. Within the range of overlap in optimum spatial frequency in the parafovea (1–2 cycles/deg), complex cells in V2 had a small but statistically significant increase in receptive field size compared to V1, and thus also in the number of cycles of the optimum grating within the field, but the increase was not accompanied by a narrowing of band width.

Our results with respect to the spatial preferences of neurones in V1 and V2 of the macaque monkey are very similar to the differences found between area 17 and area 18 in the cat. Both Movshon *et al.* (1978*a*) and Berardi *et al.* (1982) describe larger receptive field widths and a lower range of spatial frequencies in area 18 to area 17. Movshon *et al.* (1978*a*) describe the ranges of spatial frequencies in the two cortices as 'practically non-overlapping' whereas Berardi *et al.* (1982) describe a range of overlap of about 2 octaves which is similar to our extreme range of overlap; however, the primary range of overlap in the macaque monkey is about one octave.

The origin of the very low spatial frequency information in V2 remains a puzzle, given that most neurones in V1 have very little sensitivity to this range of frequencies. Perhaps this information is conveyed to V2 from the approximately 9 % of neurones in V1 with low-pass spatial frequency selectivity. Alternatively, this information could be conveyed from the inferior pulvinar, which projects densely to V2 (Trojanowski & Jacobson, 1976; Ogren & Hendrickson, 1977; Curcio & Harting, 1978), or perhaps even from the interlaminar regions of the lateral geniculate nucleus which project sparsely to V2 (Bullier & Kennedy, 1983).

Electrophysiological–psychophysical correlations. Physiological results in the macaque monkey are quite consistent with a number of psychophysical results in man. Our results, confirming those of DeValois *et al.* (1982), have shown that the mean neuronal band width tends to narrow and then flatten with increasing preferred spatial frequency in a manner very similar to the psychophysical results of Wilson, McFarlane & Phillips (1983).

Recent psychophysical studies have suggested that the lowest 'channel' with bandpass selectivity in the human fovea may be tuned to a preferred spatial frequency of 0·7 cycles/deg (Wilson *et al.* 1983). This is consistent with our physiological results that the lowest preferred spatial frequency for foveal neurones in either V1 or V2 was 0·7 cycles/deg. Other psychophysical studies which have used gratings extending just beyond the fovea have reported adaptable bandpass channels with spatial frequency preferences as low as 0·25 cycles/deg (Stromeyer, Klein, Dawson & Spillman, 1982). This result would be consistent with our finding of numerous parafoveal neurones in V2 (but not in V1) tuned to spatial frequencies of 0·25 cycles/deg.

The range of preferred spatial frequencies in the fovea of the macaque monkey

encompasses an almost 5 octave range of 0·7–16·0 cycles/deg. Watson & Robson (1981) and Wilson *et al.* (1983) have suggested that six detectors along the spatial frequency spectrum could cover this range in man. This suggestion is entirely consistent with the physiological results, given the distribution of preferred spatial frequencies and their associated band widths.

Temporal frequency selectivity of neurones in V1 and V2

We found that the majority (68%) of neurones in V1 have low-pass temporal frequency selectivity, whereas the remaining 32% have relatively broad temporal frequency selectivity with a mean band width of 2·9 octaves. On the other hand, in V2 the majority (70%) of neurones have a bandpass type of temporal selectivity, with a mean band width of 2·1 octaves, whereas only 30% have low-pass temporal selectivity. The development of more frequent and more pronounced bandpass temporal frequency selectivity is a characteristic which distinguishes V2 and V1. There are as yet no comparable studies in the macaque monkey by others with which we can compare our results. However, the differences in temporal selectivity of neurones in V1 and V2 of the macque monkey are identical to those already described in the cat by Movshon *et al.* (1978*a*) and Berardi *et al.* (1982).

The present results, combining data from both V1 and V2, suggest that there are both low-pass and bandpass temporal detectors from 0·25 to 8·0 cycles/deg. The temporal bandpass detectors for spatial frequencies of 4–8 cycles/deg are generally very broadly tuned ($\sim$ 3 octaves), but those of 0·25–2·0 cycles/deg may have substantially narrower (1·0–2·0 octaves) bandpass temporal tuning. In this lower spatial frequency range, we have found temporal frequency tuning curves with minimal overlap covering at least two distinct portions of the temporal frequency spectrum.

Electrophysiological–psychophysical correlations. These results are consistent with recent psychophysical studies in man which suggest the existence of more than one bandpass temporal frequency detector, especially in the low spatial frequency range (Watson & Robson, 1981; Bowker & Tulunay-Keesey, 1983). Our results also provide a striking neurophysiological correlate to the psychophysical result of Stromeyer *et al.* (1982) that there are both sustained and transient mechanisms for detectors tuned for spatial frequencies as low as 0·25 cycles/deg. Since the spatio-temporal threshold surfaces in man (for review, see Kelly & Burbeck, 1984) show a markedly decreased sensitivity for low spatial frequencies at low temporal frequencies, we would expect that the low-pass or sustained detectors are only excited at higher thresholds than those for the bandpass or transient detectors at these very low spatial frequencies.

Within our population of neurones in V2, cells displaying temporal bandpass selectivity were more likely to be directionally selective than cells which were not selective for temporal frequency. Moreover, these same neurones in V2 had spatial frequency preferences in the low range. These neurones in V2 have properties similar to the directionally selective detectors which psychophysicists have shown tend to have preferences for low spatial frequencies (Watson, Thompson, Murphy & Nachmias, 1980; Arditi, Anderson & Movshon, 1981).

Finally, it may be of interest that it is the temporal properties of cortical neurones rather than of geniculate neurones that match the temporal properties of the psychophysical detectors in man. The peak temporal frequencies of our cortical

neurones most often fell within the 3–8 Hz range, comparable to the preferred peak in man of about 6–8 Hz (Robson, 1966; Kelly, 1966, 1969). These peak temporal frequencies are much lower than the peak frequencies of 10–20 Hz generally found for both parvocellular and magnocellular neurones in the macaque lateral geniculate nucleus by Hicks, Lee & Vidyasagar (1983).

Functional relationship between V1 and V2

The results of the present study indicate that certain types of information which are present in V1 are further elaborated within V2. For example, the neurones of V1 are either not selective for temporal frequency or are very broadly tuned. In contrast, the neurones of V2, which are sensitive to the same range of temporal frequencies as those in V1, are much more selective. Likewise, from V1 to V2 there is a significant increase in the proportion of neurones exhibiting directional selectivity.

The present study also indicates that for certain types of information, no further elaboration occurs from V1 to V2. The most important example of this is with respect to spatial frequency selectivity: this did not increase from V1 to V2, but rather neurones in V1 and V2 were sensitive to different ranges of the spectrum. Likewise, although receptive fields were larger in V2 than in V1, this finding appeared to be associated primarily with the low preferred spatial frequencies in V2 rather than with reduced relative band widths.

Taken together, V1 and V2 contain neurones selective to an extended range of spatial frequencies with middle and high spatial frequencies in V1 and low and middle frequencies in V2. This partitioning of the spatial frequency continuum is consistent with Ginsburg's (1978) suggestion of a hierarchy of filtered images at different scales.

We sincerely thank Carol Barstow Humphrey for her dedicated technical assistance. We are grateful to Dr Peter Raudzens for teaching us the appropriate neuroanaesthetic techniques for these experiments. We sincerely thank Drs John Daugman, Norma Graham and Charles Stromeyer for their criticisms of the manuscript and helpful suggestions. This research was supported by the U.S. Public Health Service under Grant EY05156 from the National Eye Institute.

REFERENCES

Albrecht, D. G. & Hamilton, D. B. (1982). Striate cortex of monkey and cat: contrast response function. *Journal of Neurophysiology* **48**, 216–237.

Allman, J. M. & Kaas, J. H. J. (1974). The organization of the second visual area (V II) in the owl monkey: a second order transformation of the visual hemifield. *Brain Research* **76**, 247–265.

Andrews, B. W. & Pollen, D. A. (1979). Relationship between spatial frequency selectivity and receptive field profile of simple cells. *Journal of Physiology* **287**, 163–176.

Arditi, A. R., Anderson, P. A. & Movshon, J. A. (1981). Monocular and binocular detection of moving gratings. *Vision Reseach* **21**, 329–336.

Baizer, J. S., Robinson, D. L. & Dow, B. M. (1977). Visual responses of area 18 neurons in awake, behaving monkey. *Journal of Neurophysiology* **40**, 1024–1037.

Berardi, N., Bisti, S., Cattaneo, A., Fiorentini, A. & Maffei, L. (1982). Correlation between preferred orientation and spatial frequency of neurones in visual areas 17 and 18 of the cat. *Journal of Physiology* **323**, 603–618.

Bisti, S., Carmignoto, G., Galli, L. & Maffei, L. (1984). Spatial response characteristics of neurones in cat area 18 at different speeds of the visual stimulus. *Journal of Physiology* **349**, 23*P*.

Bowker, D. O. & Tulunay-Keesey, U. (1983). Sensitivity to counter-modulating gratings following spatiotemporal adaptation. *Journal of the Optical Society of America* **73**, 427–435.

BRADDICK, O., CAMPBELL, F. W. & ATKINSON, J. (1978). Channels in vision: basic aspects. In *Handbook of Sensory Physiology VIII: Perception*, ed. HELD, R., LIEBOWITZ, H. & TEUBER, H. L., pp. 3–37. Heidelberg: Springer.

BULLIER, J. & KENNEDY, H. (1983). Projection of the lateral geniculate nucleus onto cortical area V2 in the macaque monkey. *Experimental Brain Research* **53**, 168–172.

BURR, D. C. & ROSS, J. (1982). Contrast sensitivity at high velocities. *Vision Research* **22**, 479–484.

CURCIO, C. A. & HARTING, J. K. (1978). Organization of pulvinar afferents to area 18 in the squirrel monkey: evidence for stripes. *Brain Research* **143**, 155–161.

DANIEL, M. & WHITTERIDGE, D. (1961). The representation of the visual field on the cerebral cortex in monkeys. *Journal of Physiology* **159**, 203–221.

DEAN, A. F. & TOLHURST, P. J. (1983). On the distinctiveness of simple and complex cells in the visual cortex of the cat. *Journal of Physiology* **344**, 305–325.

DESIMONE, R., FLEMING, J. & GROSS, C. G. (1980). Prestriate afferents to inferior temporal cortex: an HRP study. *Brain Research* **184**, 41–55.

DEVALOIS, R. L., ALBRECHT, D. G. & THORELL, L. G. (1982). Spatial frequency selectivity of cells in macaque visual cortex. *Vision Research* **22**, 545–559.

DEVALOIS, R. L., MORGAN, H. C. & SNODDERLY, D. M. (1974). Psychophysical studies of monkey vision. III. Spatial luminance contrast sensitivity tests of macaque and human observers. *Vision Research* **14**, 75–82.

DEVALOIS, K. K. & TOOTELL, R. B. H. (1983). Spatial frequency-specific inhibition in cat striate cortex cells. *Journal of Physiology* **336**, 359–376.

DOW, B. M. (1974). Functional classes of cells and their laminar distribution in monkey visual cortex. *Journal of Neurophysiology* **37**, 927–946.

GATTASS, R., GROSS, C. G. & SANDELL, J. H. (1981). Visual topography of V2 in the macaque. *Journal of Comparative Neurology* **201**, 519–539.

GINSBURG, A. P. (1978). Visual information processing based on spatial filters constrained by biological data. Ph.D. Thesis, University of Cambridge.

GLEZER, V. D., TSCHERBACH, T. A., GAUSELMAN, V. E. & BONDARKO, V. M. (1980). Linear and non-linear properties of simple and complex receptive fields in area 17 of the cat visual cortex. A model of the field. *Biological Cybernetics* **37**, 195–208.

HENDRICKSON, A. E., WILSON, J. R. & OGREN, M. P. (1978). The neuroanatomical organization of pathways between the dorsal lateral geniculate nucleus and visual cortex in old world and new world primates. *Journal of Comparative Neurology* **182**, 123–136.

HICKS, T. P., LEE, B. B. & VIDYASAGAR, T. R. (1983). The responses of cells in the macaque lateral geniculate nucleus to sinusoidal gratings. *Journal of Physiology* **337**, 183–200.

HOLUB, R. A. & MORTON-GIBSON, M. (1981). Response of visual cortical neurons of the cat to moving sinusoidal gratings: response contrast functions and spatiotemporal interactions. *Journal of Neurophysiology* **46**, 1244–1259.

HUBEL, D. H. & WIESEL, T. N. (1962). Receptive fields, binocular interaction and functional architecture in the cat's visual cortex. *Journal of Physiology* **160**, 106–154.

HUBEL, D. H. & WIESEL, T. N. (1968). Receptive fields and functional architecture of monkey striate cortex. *Journal of Physiology* **195**, 215–243.

IKEDA, H. & WRIGHT, M. J. (1975). Spatial and temporal properties of "sustained" and "transient" neurones in area 17 of the cat's visual cortex. *Experimental Brain Research* **22**, 363–383.

KELLY, D. H. (1966). Frequency doubling in visual responses. *Journal of the Optical Society of America* **56**, 1628.

KELLY, D. H. (1969). Flickering patterns and lateral inhibition. *Journal of the Optical Society of America* **59**, 1361–1369.

KELLY, D. H. & BURBECK, C. A. (1984). Critical problems in spatial vision. *CRC Critical Reviews in Biomedical Engineering* **10**, 125–177.

KULIKOWSKI, J. J. & BISHOP, P. O. (1982). Silent periodic cells in the cat striate cortex. *Vision Research* **22**, 191–201.

KULIKOWSKI, S., MARCELJA, S. & BISHOP, P. O. (1982). Theory of spatial position and spatial frequency relations in the receptive fields of simple cells in the visual cortex. *Biological Cybernetics* **43**, 182–198.

LUND, J. S., HENDRICKSON, A. E., OGREN, M. P. & TOBIN, E. A. (1981). Anatomical organization of primate visual cortex area V II. *Journal of Comparative Neurology* **202**, 19–45.

MAFFEI, L. & FIORENTINI, A. (1973). The visual cortex as a spatial frequency analyzer. *Vision Research* **13**, 1255–1267.

MAFFEI, L. & FIORENTINI, A. (1976). The unresponsive regions of visual cortical receptive fields. *Vision Research* **16**, 1131–1139.

MAUNSELL, J. H. R. & VAN ESSEN, D. C. (1983). The connections of the middle temporal visual area (MT) and their relationship to a cortical hierarchy in the macaque monkey. *Journal of Neuroscience* **3**, 2563–2586.

MOVSHON, J. A., THOMPSON, I. D. & TOLHURST, D. J. (1978*a*). Spatial and temporal contrast sensitivity of neurones in area 17 and 18 of the cat's visual cortex. *Journal of Physiology* **283**, 101–120.

MOVSHON, J. A., THOMPSON, I. D. & TOLHURST, D. J. (1978*b*). Spatial summation in the receptive fields of simple cells in the cat's striate cortex. *Journal of Physiology* **283**, 53–77.

MOVSHON, J. A., THOMPSON, I. D. & TOLHURST, D. J. (1978*c*). Receptive field organization of complex cells in the cat's striate cortex. *Journal of Physiology* **283**, 79–99.

MOVSHON, J. A. & TOLHURST, D. J. (1975). On the response linearity of neurons in cat visual cortex. *Journal of Physiology* **249**, 56–57.

OGREN, M. P. & HENDRICKSON, A. E. (1977). The distribution of pulvinar terminals in visual areas 17 and 18 of the monkey. *Brain Research* **137**, 343–350.

POGGIO, G. F. (1972). Spatial properties of neurones in striate cortex of unanesthetized macaque monkey. *Investigative Ophthalmology* **11**, 368–377.

POLLEN, D. A., ANDREWS, B. W. & FELDON, S. E. (1978). Spatial frequency selectivity of periodic complex cells in the visual cortex of the cat. *Vision Research* **18**, 665–682.

POLLEN, D. A. & RONNER, S. F. (1983). Visual cortical neurons as localized spatial frequency filters. *IEEE Trans. Systems, Man and Cybernetics* **13**, 907–915.

ROBSON, J. G. (1966). Spatial and temporal contrast-sensitivity functions of the visual system. *Journal of the Optical Society of America* **56**, 1141–1142.

ROBSON, J. G. (1975). Receptive fields: neural representation of the spatial and intensive attributes of the visual image. In *Handbook of Perception*, vol. 5, ed. CARTERETTE, E. C. & FRIEDMAN, M. P., pp. 81–116. New York: Academic Press.

ROCKLAND, K. S. & PANDYA, D. N. (1981). Cortical connections of the occipital lobe in the rhesus monkey: interconnections between areas 17, 18, 19 and the superior temporal sulcus. *Brain Research* **212**, 249–270.

SAKITT, B. & BARLOW, H. B. (1982). A model for the economic cortical encoding of the visual image. *Biological Cybernetics* **43**, 97–108.

SCHILLER, P. H., FINLAY, B. L. & VOLMAN, S. F. (1976*a*). Quantitative studies of single-cell properties in monkey striate cortex. III. Spatial frequency. *Journal of Neurophysiology* **39**, 1334–1351.

SCHILLER, P. H., FINLAY, B. L. & VOLMAN, S. F. (1976*b*). Quantitative studies of single-cell properties in monkey striate cortex. I. Spatiotemporal organization of receptive fields. *Journal of Neurophysiology* **39**, 1288–1319.

SCHILLER, P. H. & MALPELI, J. G. (1977). The effect of striate cortex cooling on area 18 cells in the monkey. *Brain Research* **126**, 366–369.

STROMEYER III, C. F., KLEIN, S., DAWSON, B. M. & SPILLMAN, L. (1982). Low spatial-frequency channels in human vision: adaptation and masking. *Vision Research* **22**, 225–233.

TALBOT, S. A. & MARSHALL, W. H. (1941). Physiological studies on neural mechanisms of visual localization and discrimination. *American Journal of Ophthalmology* **24**, 1255–1263.

TOLHURST, D. J. & MOVSHON, J. A. (1975). Spatial and temporal contrast sensitivity of striate cortical neurons. *Nature* **257**, 674–675.

TOOTELL, R. B. H., SILVERMAN, M. S., DEVALOIS, R. L. & JACOBS, G. H. (1983). Functional organization of the second cortical visual area in primates. *Science* **220**, 737–739.

TROJANOWSKI, J. Q. & JACOBSON, S. (1976). Areal and laminar distribution of some pulvinar cortical efferents in rhesus monkey. *Journal of Comparative Neurology* **169**, 371–392.

VAN ESSEN, D. C. & ZEKI, S. M. (1978). The topographic organization of rhesus monkey prestriate cortex. *Journal of Physiology* **277**, 193–226.

WATSON, A. B., THOMPSON, P. G., MURPHY, B. J. & NACHMIAS, J. (1980). Summation and discrimination of gratings moving in opposite directions. *Vision Research* **20**, 341–347.

WATSON, A. B. & ROBSON, J. G. (1981). Discrimination at threshold: labelled detectors in human vision. *Vision Research* **21**, 1115–1122.

WELLER, R. E. & KAAS, J. H. (1983). Retinotopic patterns of connections of area 17 with visual areas V II and MT in macaque monkeys. *Journal of Comparative Neurology* **220**, 253–279.

WILSON, H. R. (1980). Spatiotemporal characterization of a transient mechanism in the human visual system. *Vision Research* **20**, 443–452.

WILSON, H. R., MCFARLANE, D. K. & PHILLIPS, G. C. (1983). Spatial frequency tuning of orientation selective units estimated by oblique masking. *Vision Research* **23**, 873–882.